THE UNIVERSITY OF SYDNEY

ARC CENTRE OF EXCELLENCE FOR DARK MATTER

Axion clumps, streams, and voids

Ciaran O'Hare
University of Sydney

Phys. Rev. Lett. 133, 081001 (2024)

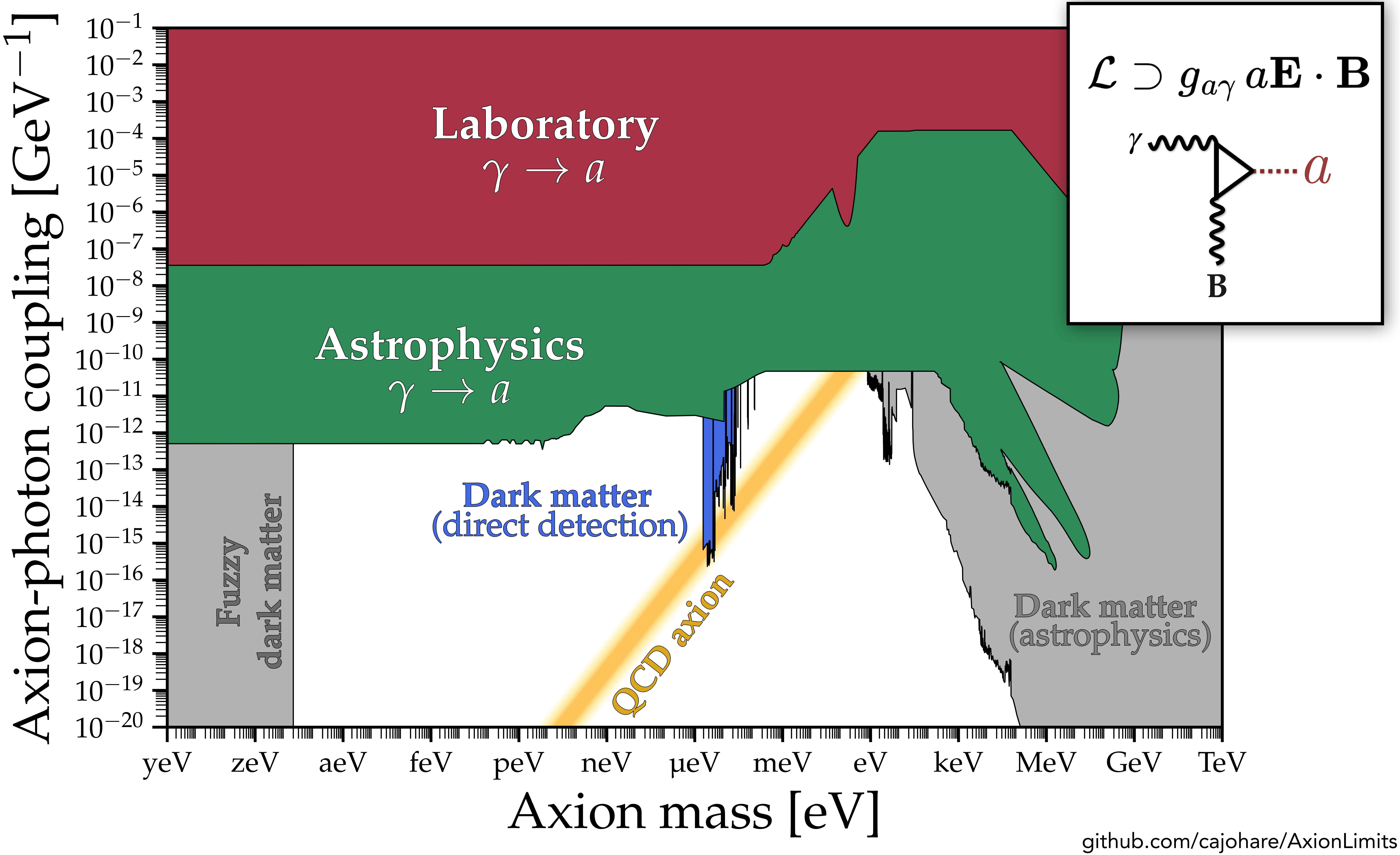

Laboratory
$\gamma \to a$
Astrophysics
$\gamma \to a$
Dark matter
(direct detection)
QCD axion
Fuzzy
dark matter
Dark matter
(astrophysics)
$\mathcal{L} \supset g_{a\gamma}\, a\mathbf{E}\cdot\mathbf{B}$
γ
a
B
Axion-photon coupling [GeV^{-1}]
10^{-1}
10^{-2}
10^{-3}
10^{-4}
10^{-5}
10^{-6}
10^{-7}
10^{-8}
10^{-9}
10^{-10}
10^{-11}
10^{-12}
10^{-13}
10^{-14}
10^{-15}
10^{-16}
10^{-17}
10^{-18}
10^{-19}
10^{-20}
yeV
zeV
aeV
feV
peV
neV
µeV
meV
eV
keV
MeV
GeV
TeV
Axion mass [eV]
github.com/cajohare/AxionLimits

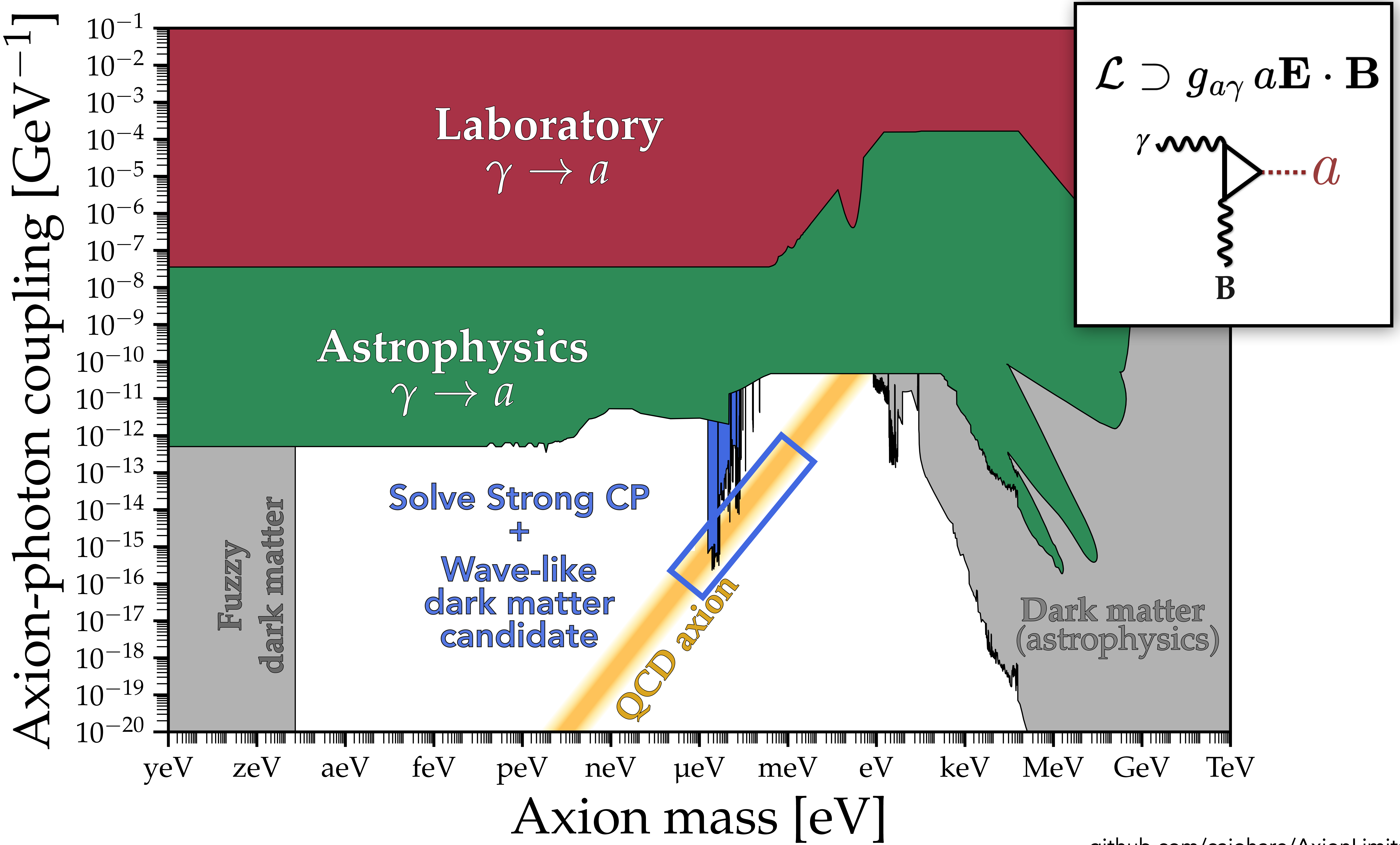

github.com/cajohare/AxionLimits

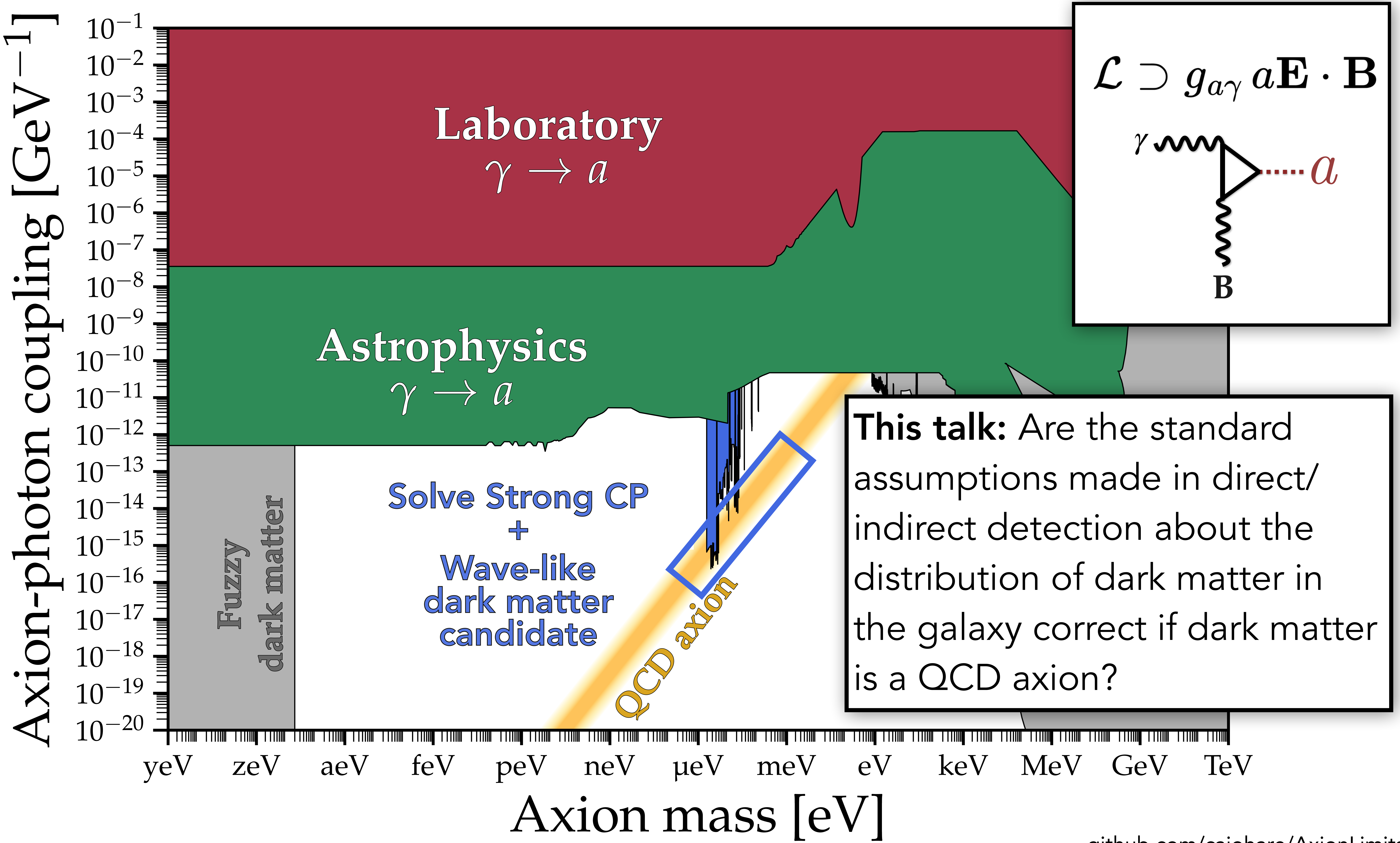

This talk: Are the standard assumptions made in direct/indirect detection about the distribution of dark matter in the galaxy correct if dark matter is a QCD axion?

github.com/cajohare/AxionLimits

Production of QCD axion DM: The misalignment mechanism

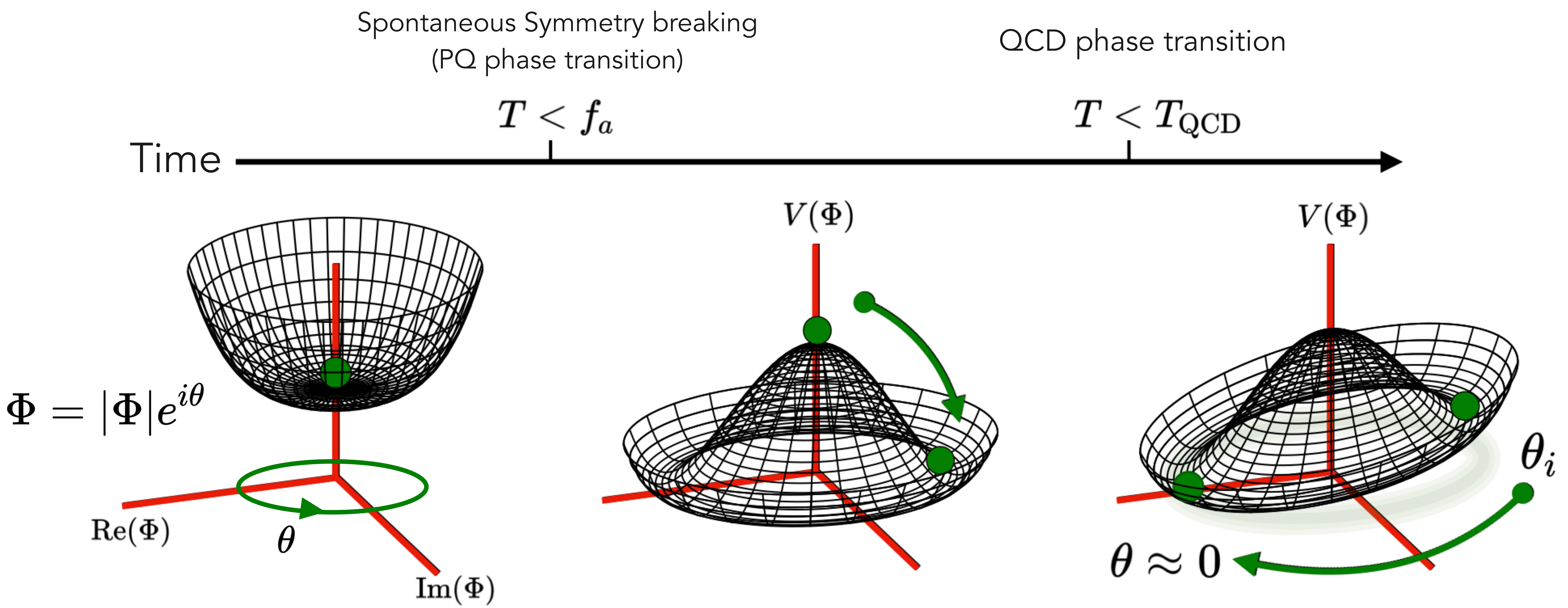

Present-day abundance of axions controlled by initial "misalignment" angle: $\Omega_a \propto \theta_i^2$

QCD axion abundance

- Accounting for the temperature-dependence of axion mass (topological susceptibility) we get:

$$\Omega_a h^2 \approx 0.12\,\theta_i^2 \left(\frac{7.26\,\mu\mathrm{eV}}{m_a}\right)^{\frac{n+6}{n+4}}$$

where $n \sim 8$ (from Lattice QCD, e.g. 1606.07494)

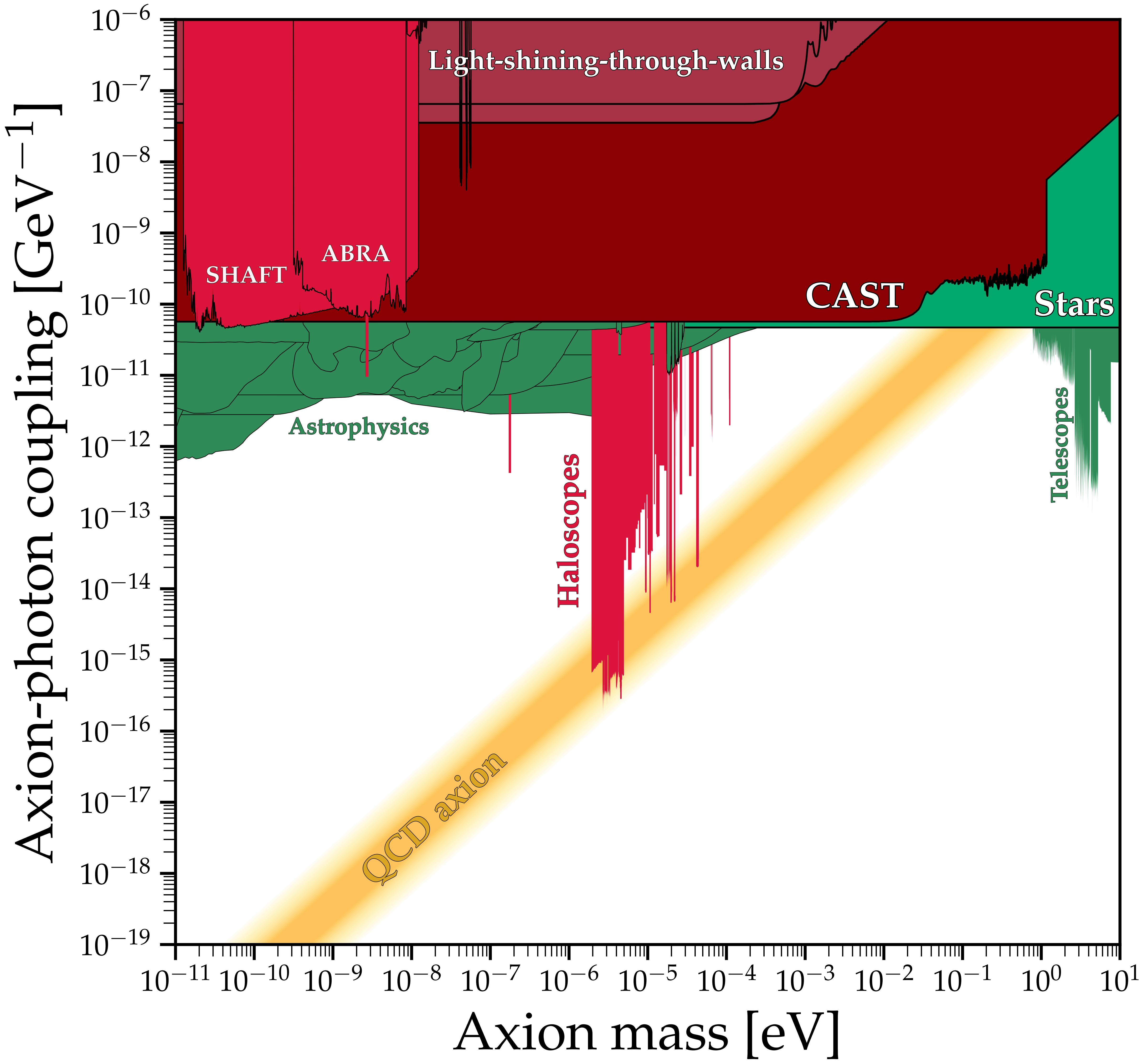

QCD axion abundance

- Accounting for the temperature-dependence of axion mass (topological susceptibility) we get:

$$\Omega_a h^2 \approx 0.12\, \theta_i^2 \left(\frac{7.26\, \mu\mathrm{eV}}{m_a} \right)^{\frac{n+6}{n+4}}$$

where $n \sim 8$ (from Lattice QCD, e.g. 1606.07494)

- Explaining 100% axion DM with $\theta \sim \mathcal{O}(1)$ leads to "classic QCD axion window": $\mathcal{O}$(1—10) μeV

→ **what should we be picking for θ_i ?**

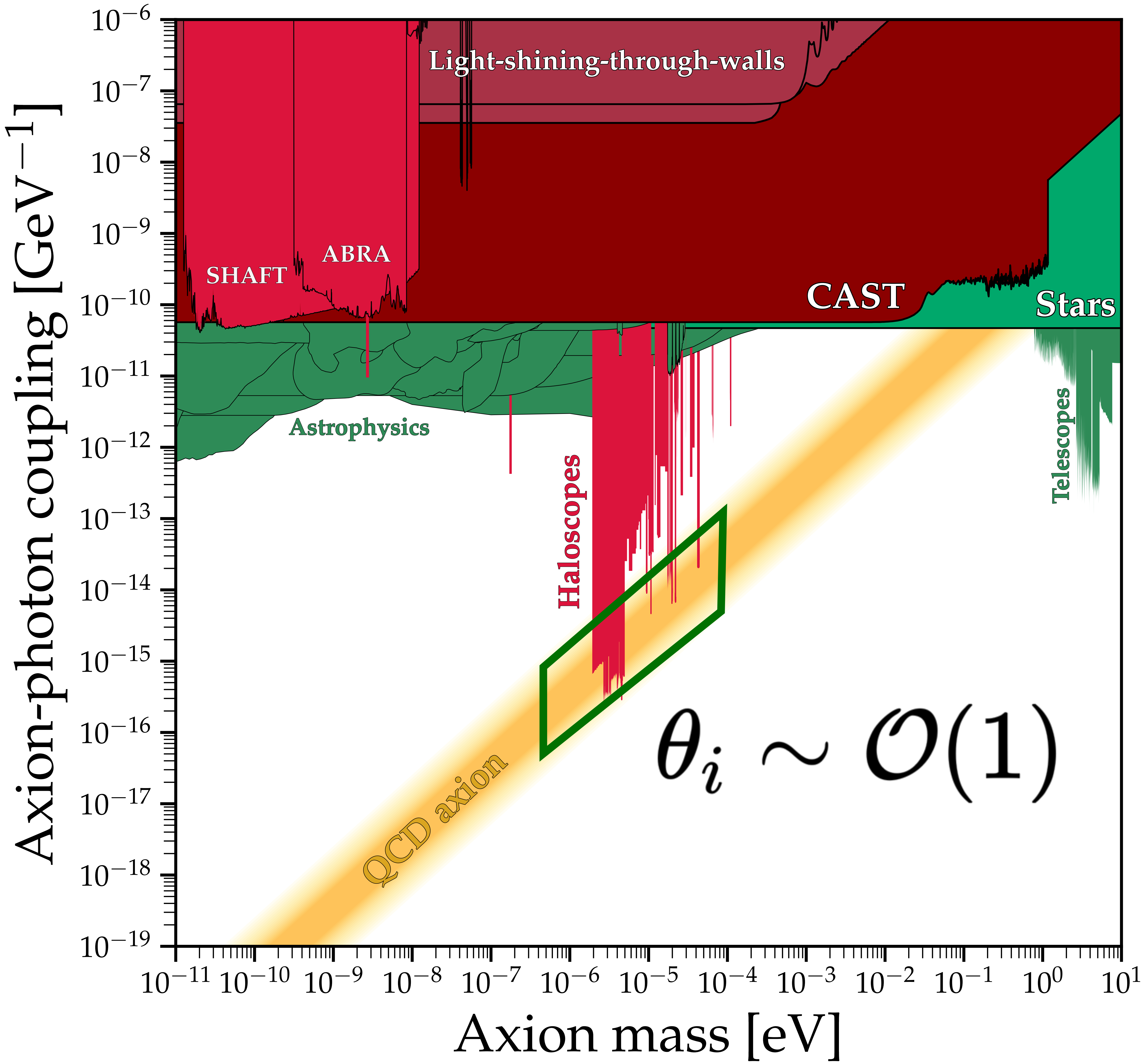

When did inflation happen?

Scenario 1:
SSB *before* inflation

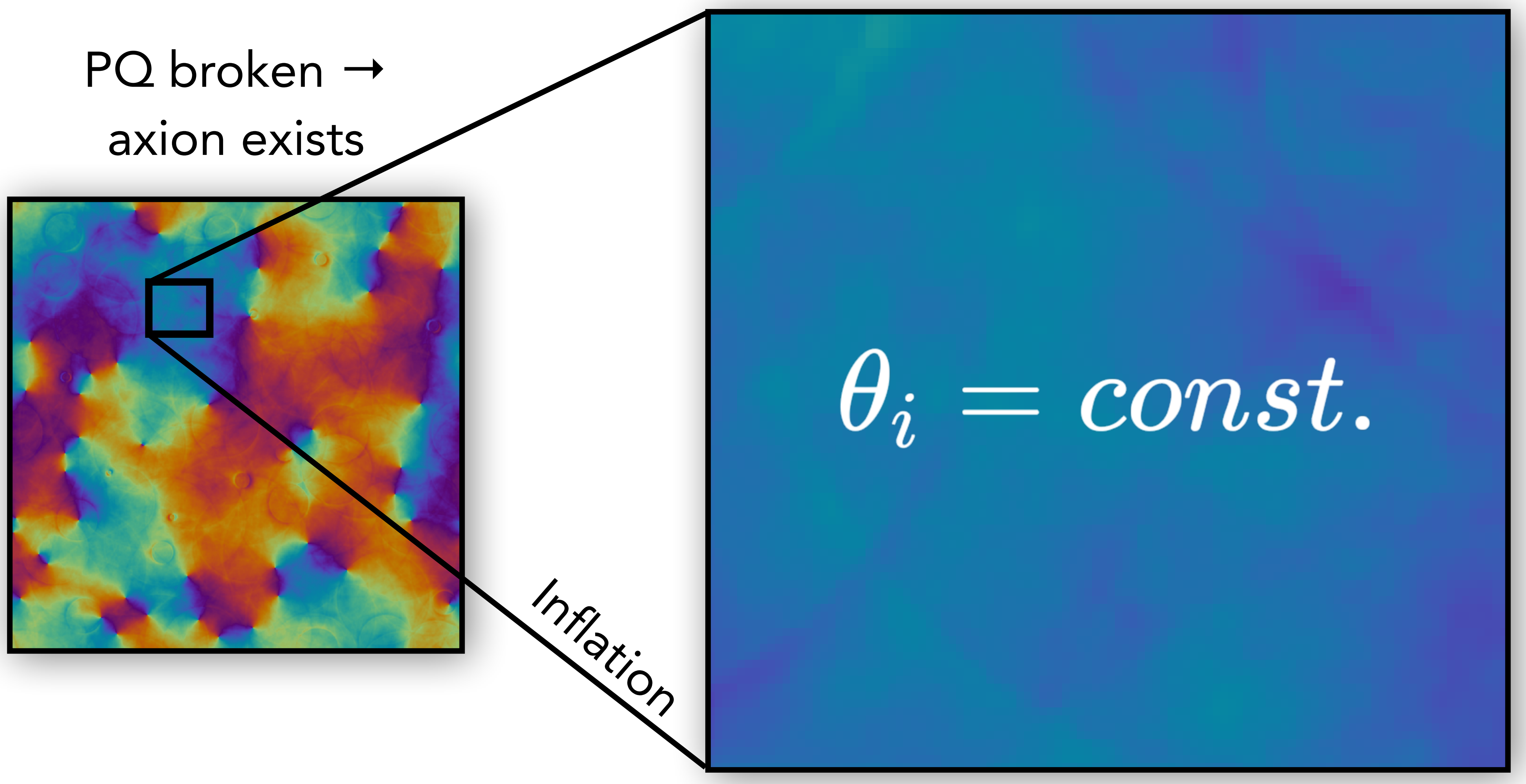

Pre-inflationary scenario

When did inflation happen?

Scenario 1:
SSB *before* inflation

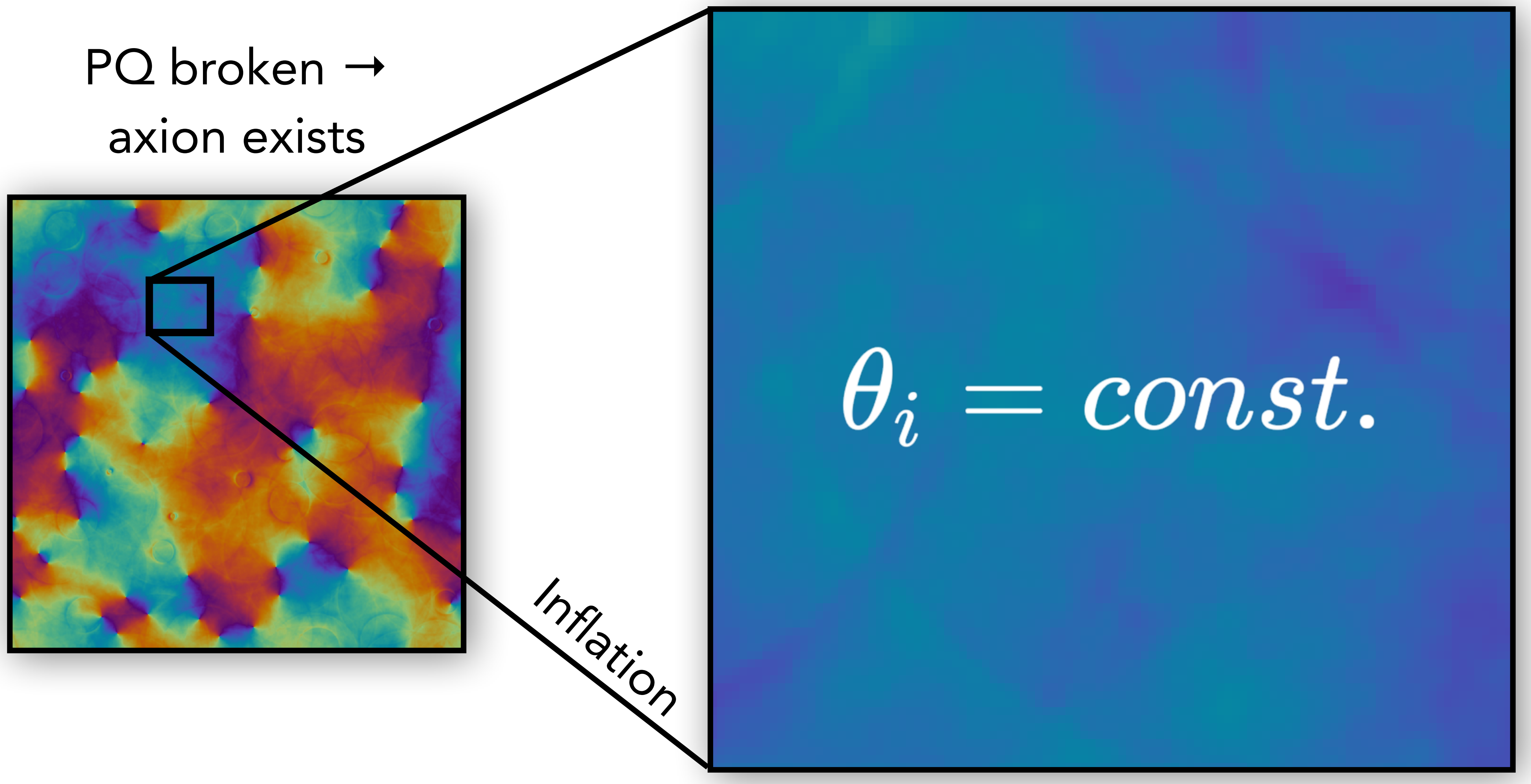

Pre-inflationary scenario

Scenario 2:
SSB *after* inflation

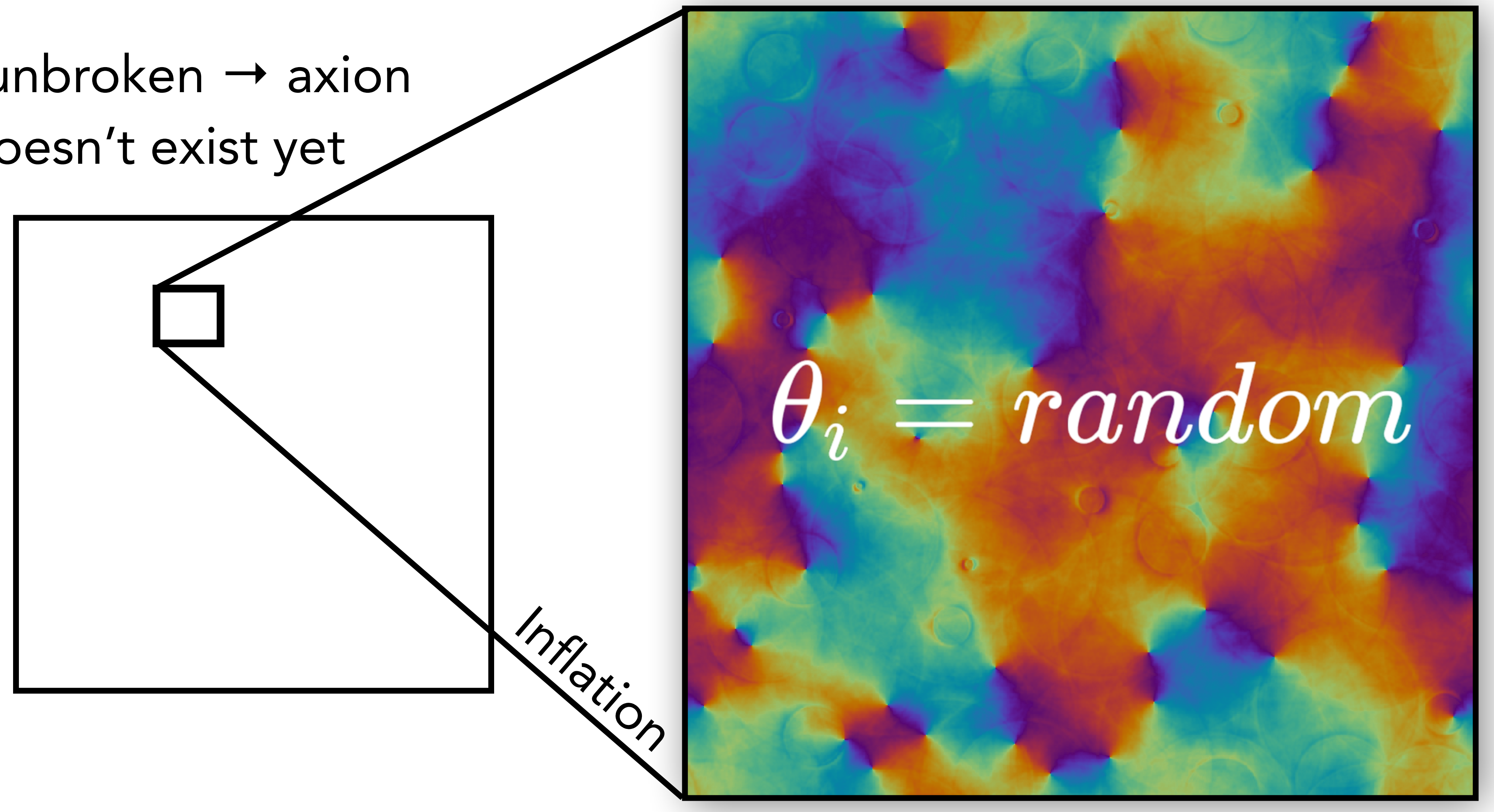

Post-inflationary scenario

Scenario II: *Post*-inflationary axions

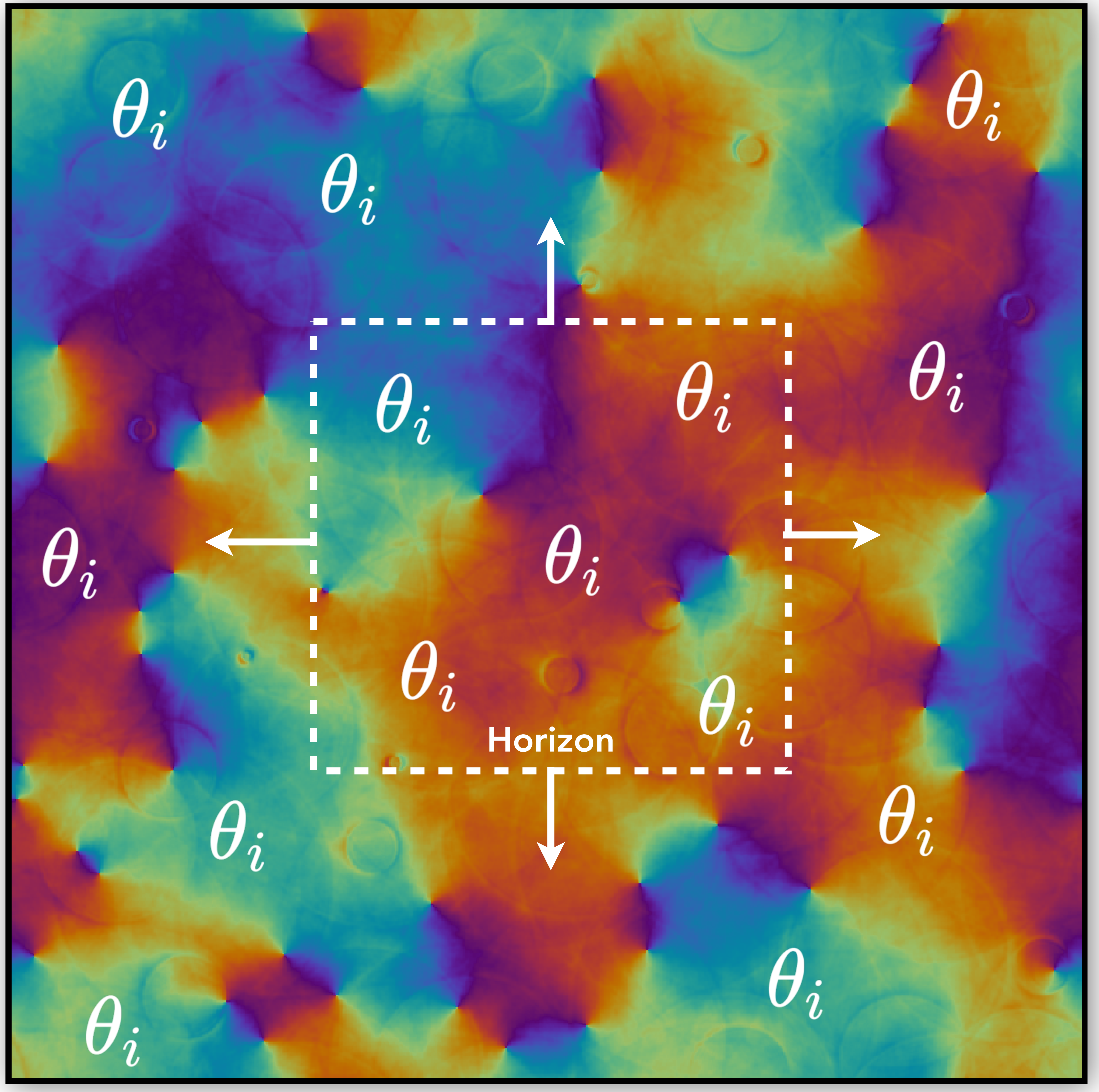

Assume inflation has already happened when axion is born

→ Universe filled with many patches of different θ_i

→ Patches come into contact as horizon grows.

Post-inflationary scenario

- We have an ensemble of every possible θ_i sampled across our Universe.
- Stochastic average: $\langle\theta_i^2\rangle \approx (\pi/\sqrt{3})^2$

$$\Omega_a h^2 \approx 0.12 \frac{\langle\theta_i^2\rangle}{(1.81)^2}\left(\frac{20\mu\text{eV}}{m_a}\right)^{\frac{n+6}{n+4}}$$

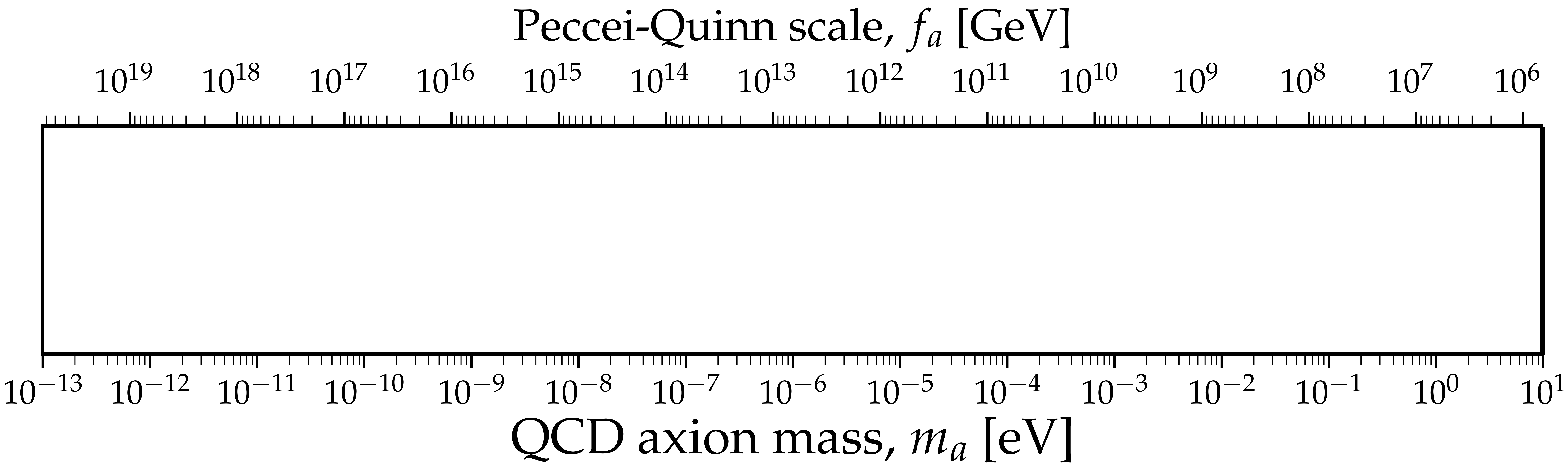

Post-inflationary scenario

- We have an ensemble of every possible θ_i sampled across our Universe.
- Stochastic average: $\langle \theta_i^2 \rangle \approx (\pi/\sqrt{3})^2$

$$\Omega_a h^2 \approx 0.12 \frac{\langle \theta_i^2 \rangle}{(1.81)^2} \left(\frac{20\mu\text{eV}}{m_a} \right)^{\frac{n+6}{n+4}}$$

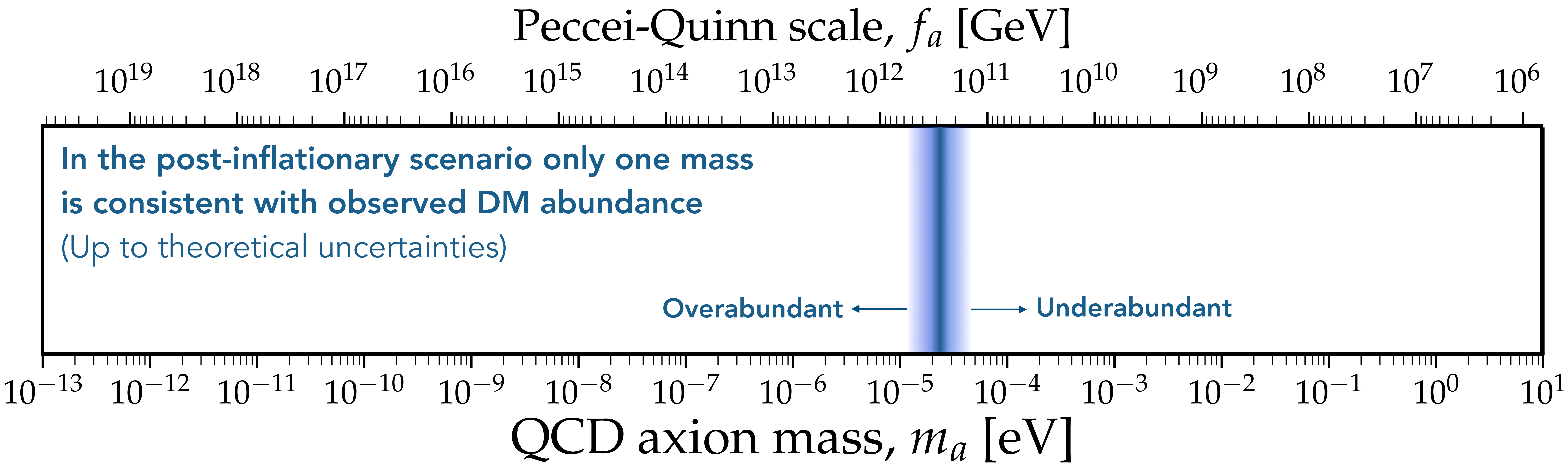

Uncertainties: $\nabla\theta$ and topological defects

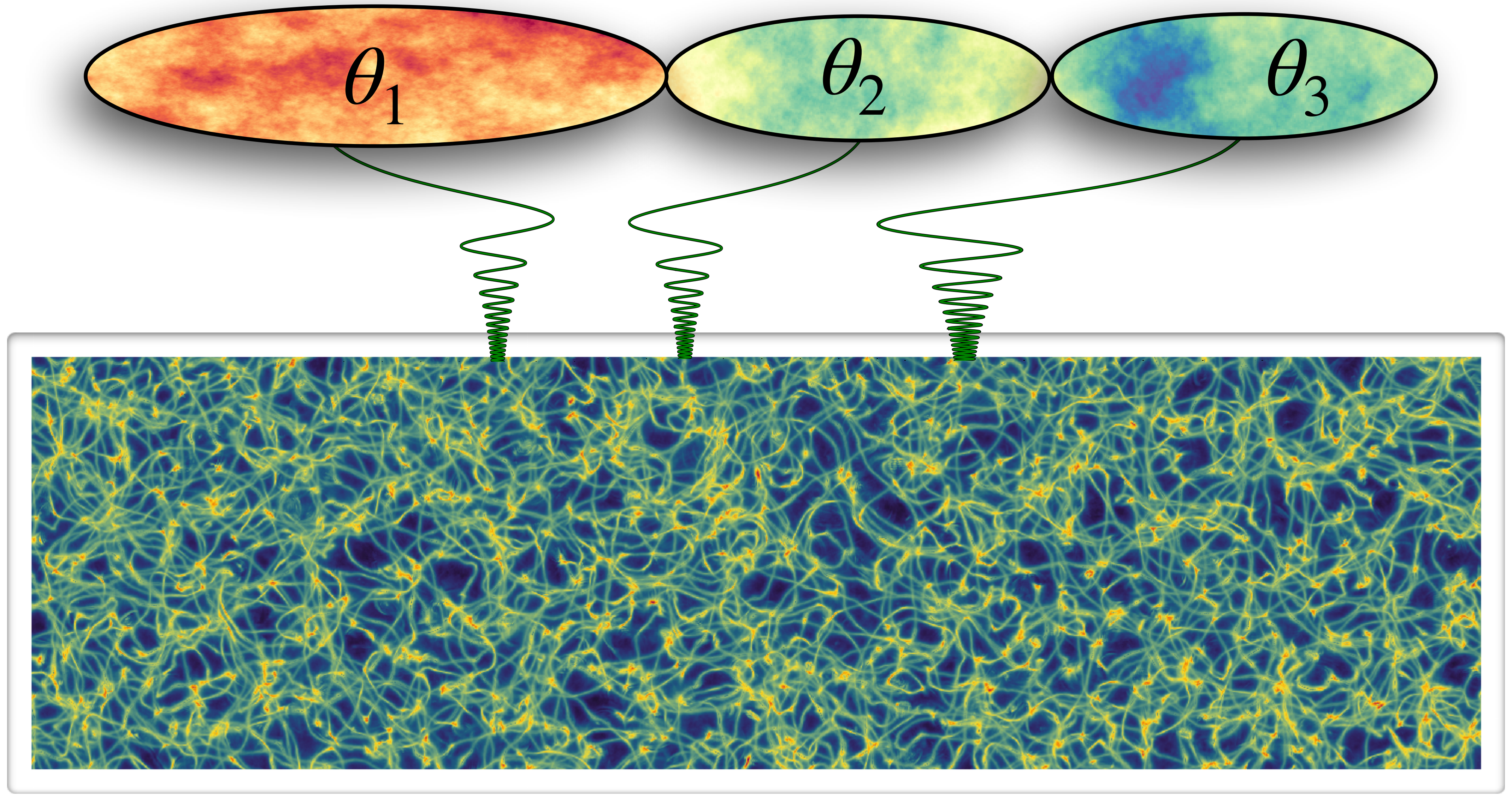

Different patches meet up
→ Field gradients!

$$\longleftarrow \quad \ddot{\theta} + 3H\dot{\theta} - \frac{1}{a^2}\nabla^2\theta + m_a^2\theta = 0$$

Uncertainties: $\nabla\theta$ and topological defects

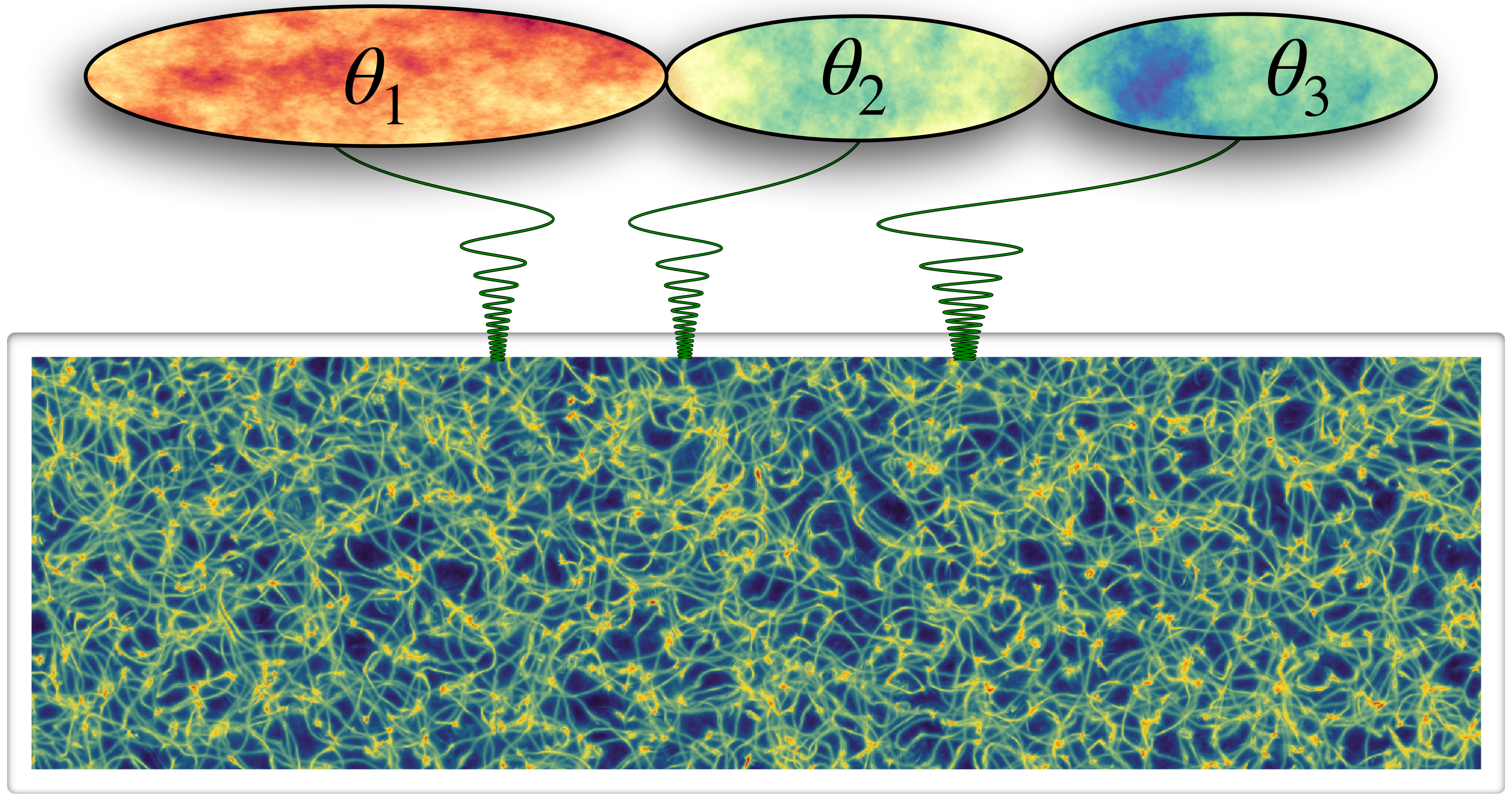

Different patches meet up
→ Field gradients!

$$\longleftarrow \quad \ddot{\theta} + 3H\dot{\theta} \boxed{- \frac{1}{a^2}\nabla^2\theta} + m_a^2\theta = 0$$

⇒ **Cosmic strings**
from axion field
winding around 2π

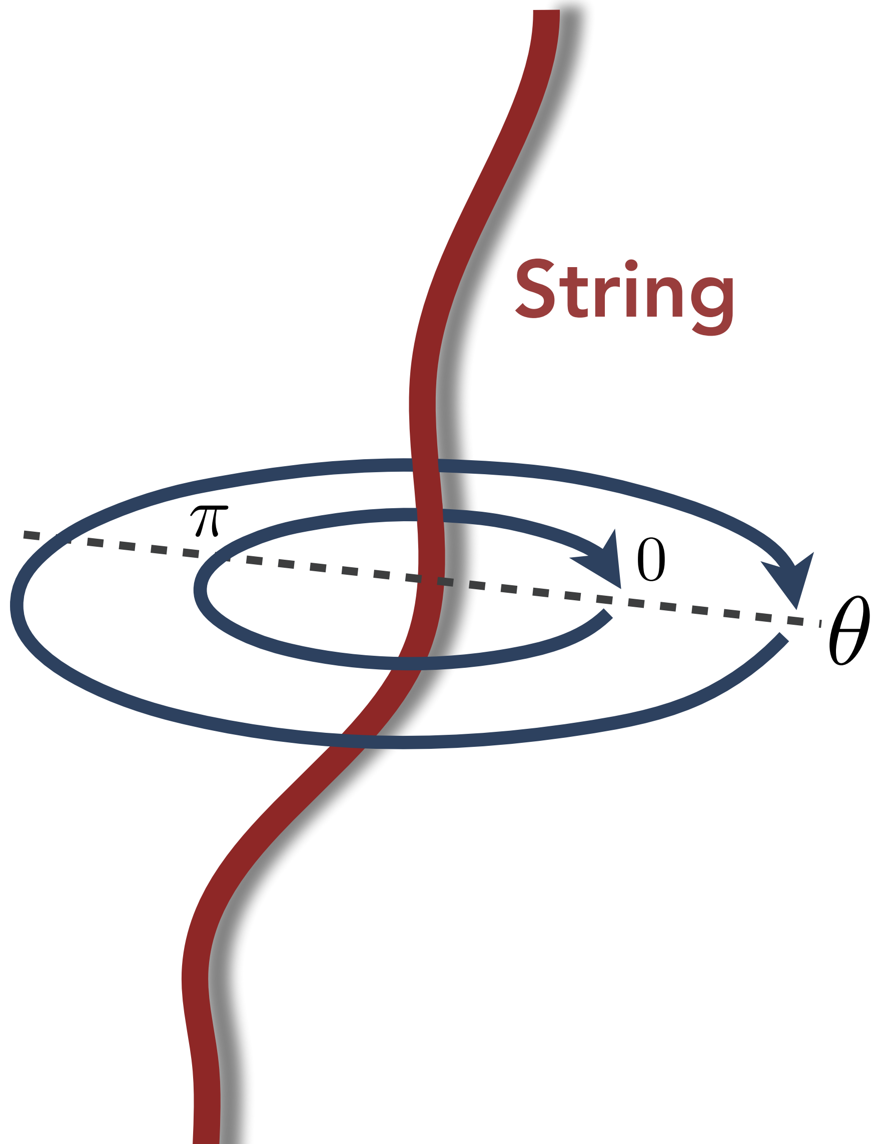

Uncertainties: $\nabla\theta$ and topological defects

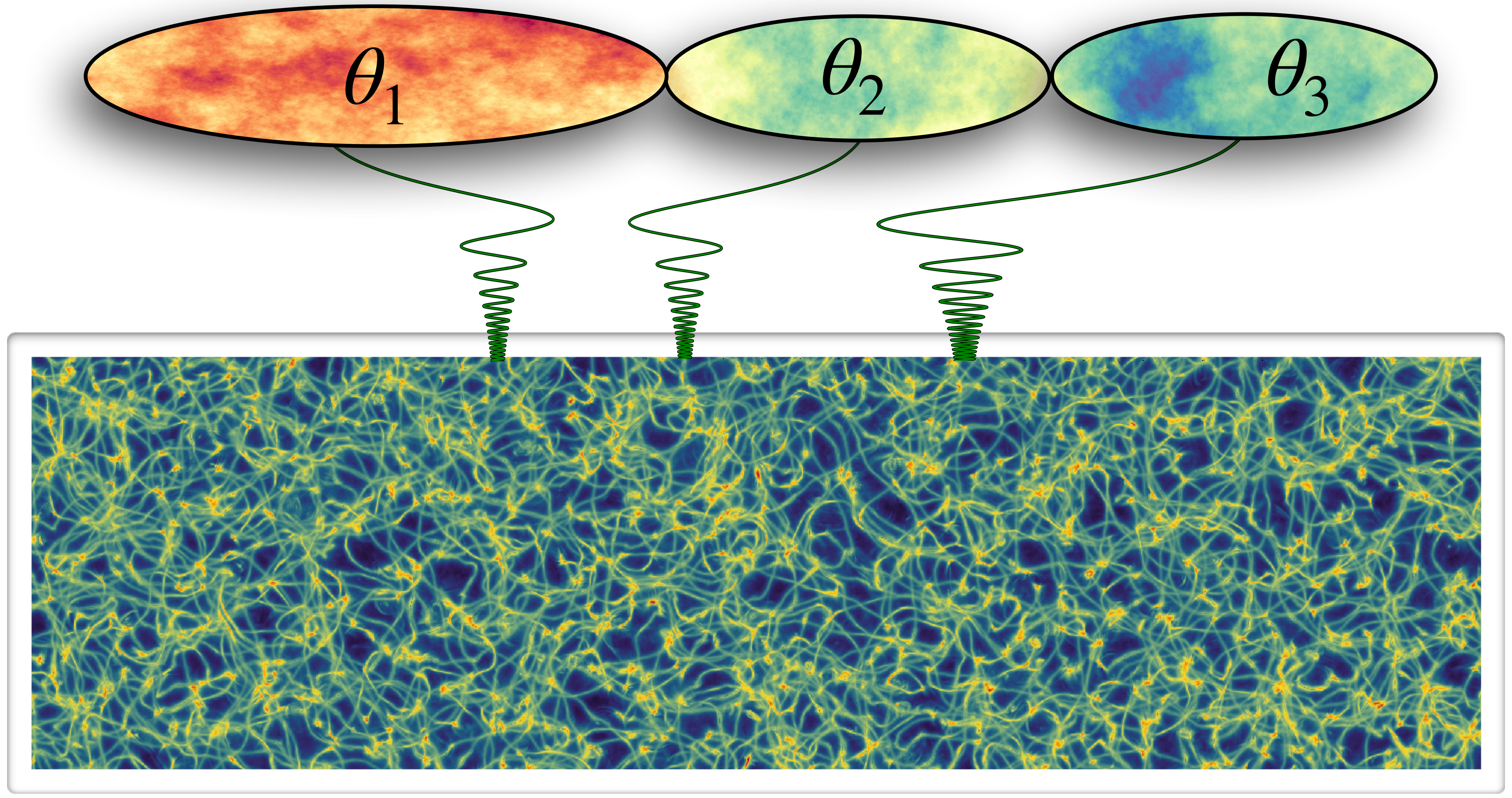

Different patches meet up

→ Field gradients!

$$\longleftarrow \quad \ddot{\theta} + 3H\dot{\theta} - \frac{1}{a^2}\nabla^2\theta + m_a^2\theta = 0$$

⇒ **Cosmic strings**

from axion field winding around 2π

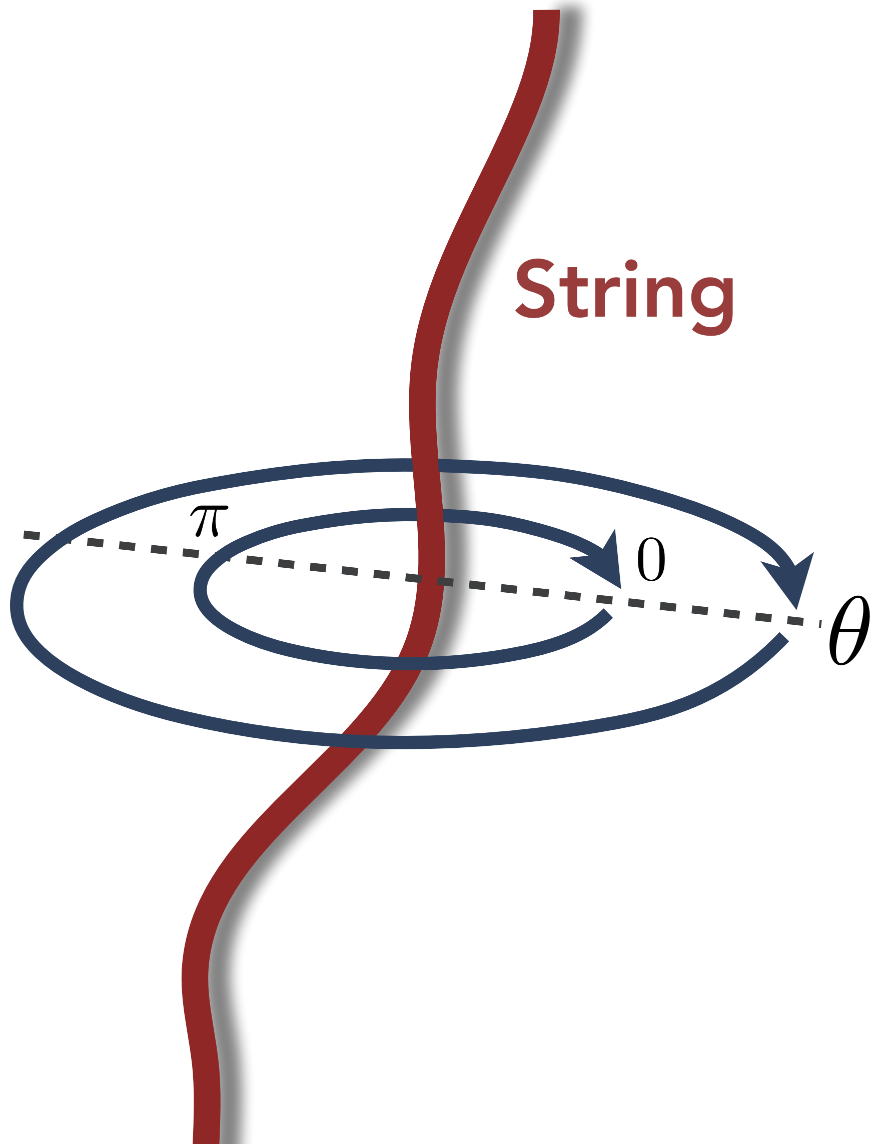

⇒ **Domain walls**

between true/false vacuum (0 and π)

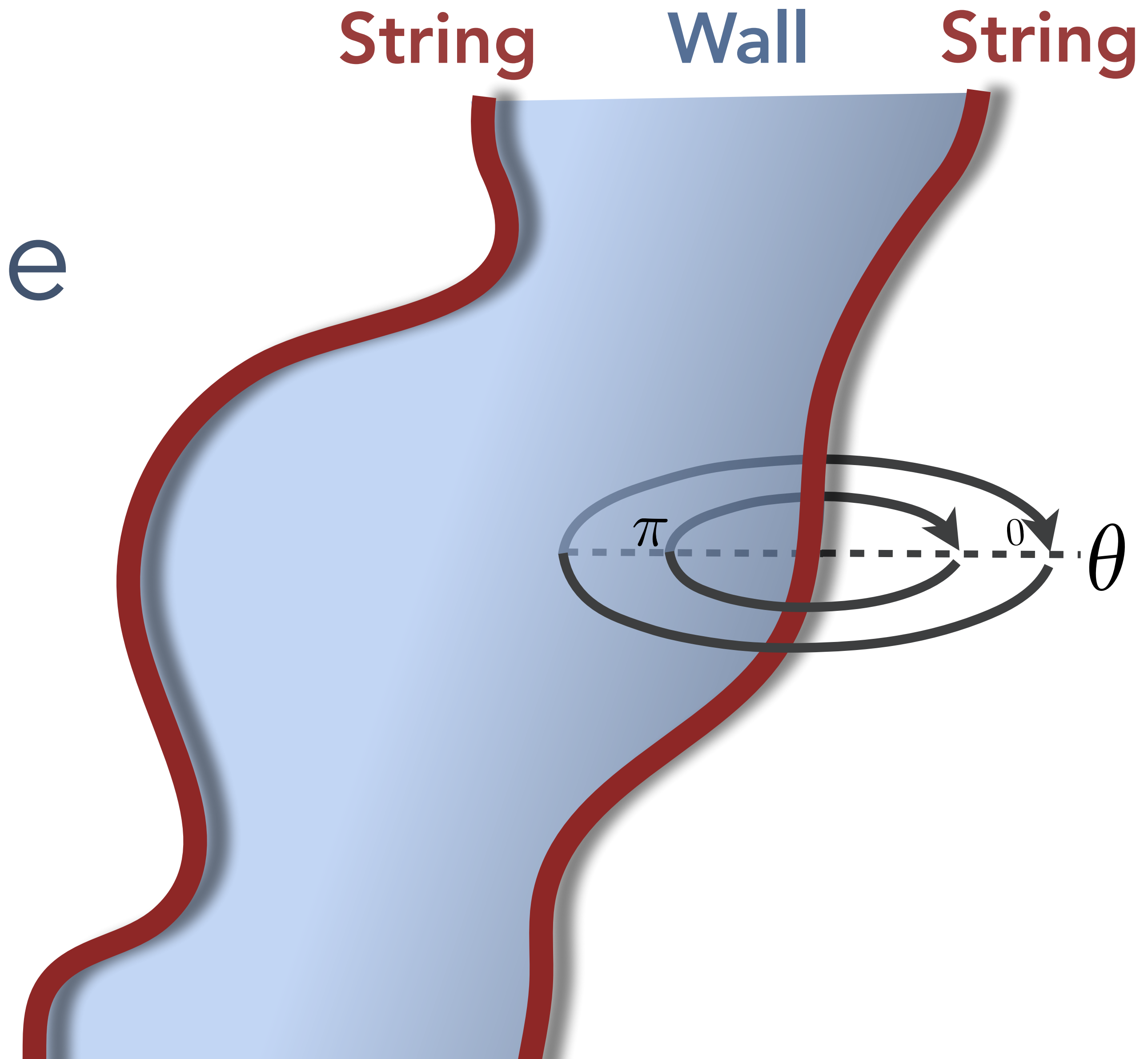

Evolution of the axion field in the post-inflationary scenario

Projection through 3D co-moving box, coloured by integrated axion energy density:

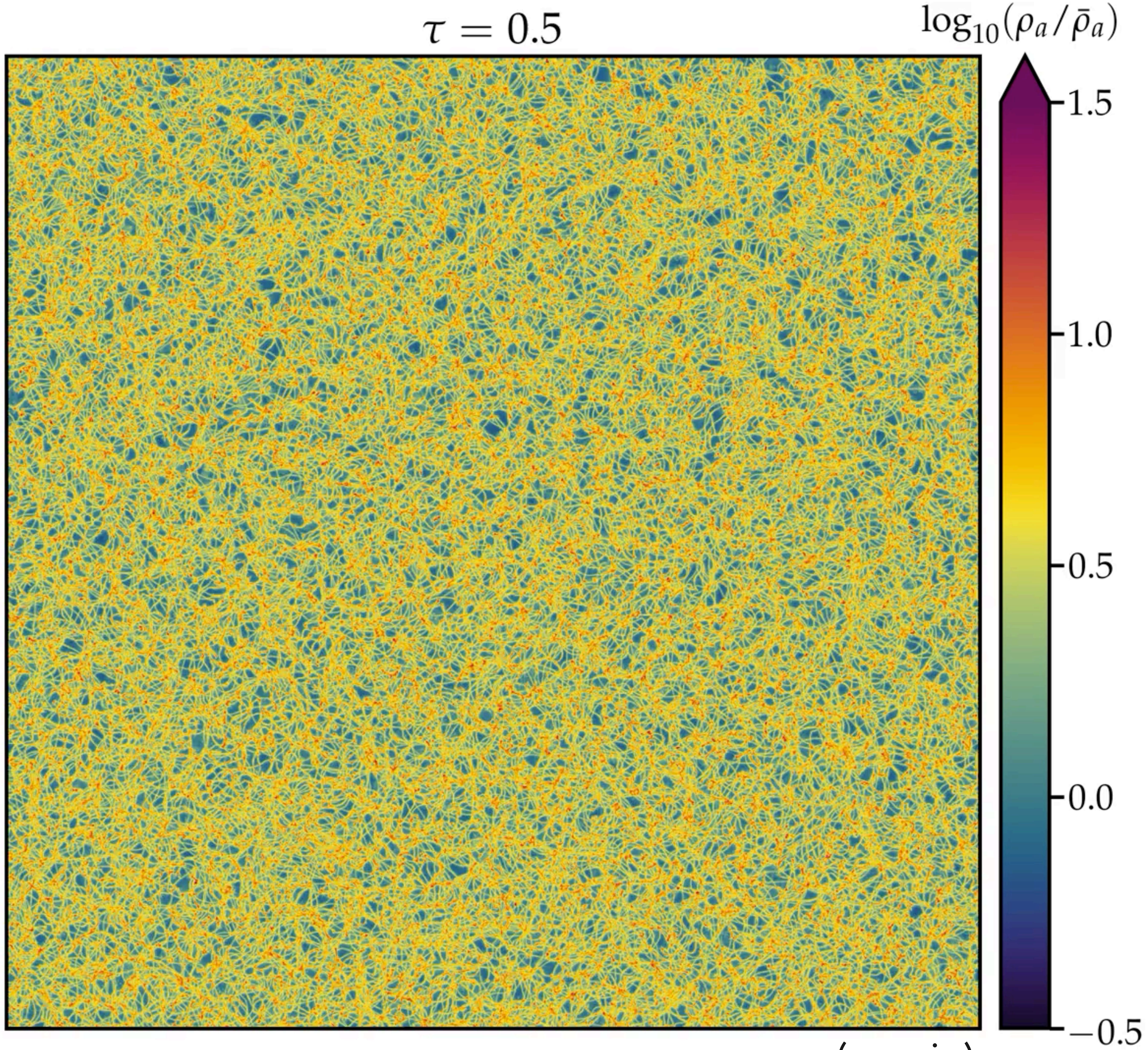

(movie)

Evolution of the axion field in the post-inflationary scenario

Projection through 3D co-moving box, coloured by integrated axion energy density:

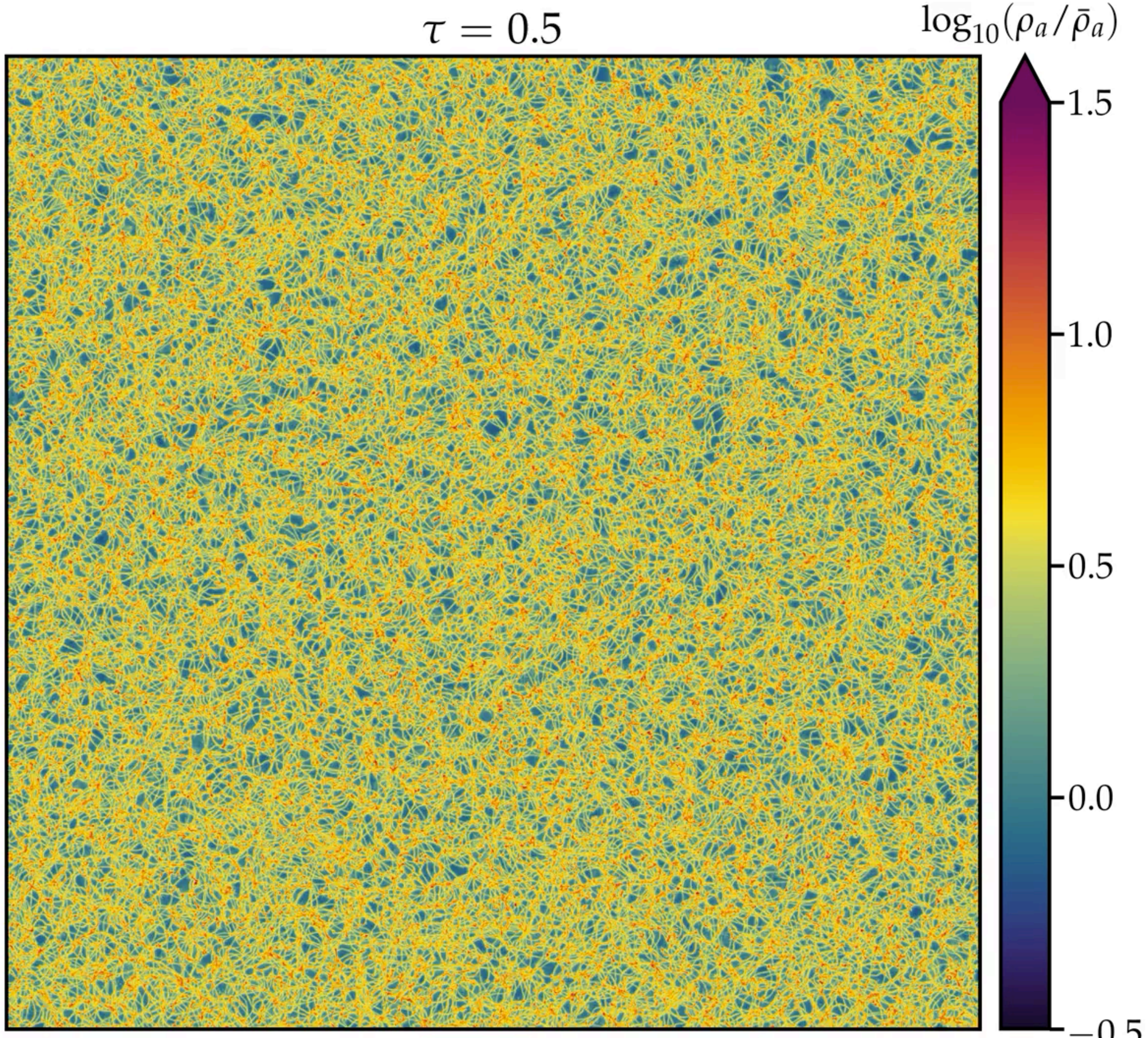

(movie)

Gravitational collapse in the post-inflationary scenario

Axion distribution is highly *inhomogeneous:* isocurvature density fluctuations on scales set by horizon-size at $T_{\rm QCD}$. Collapse and growth of these fluctuations leads to enhanced small-scale dark matter structure: "**axion miniclusters**"

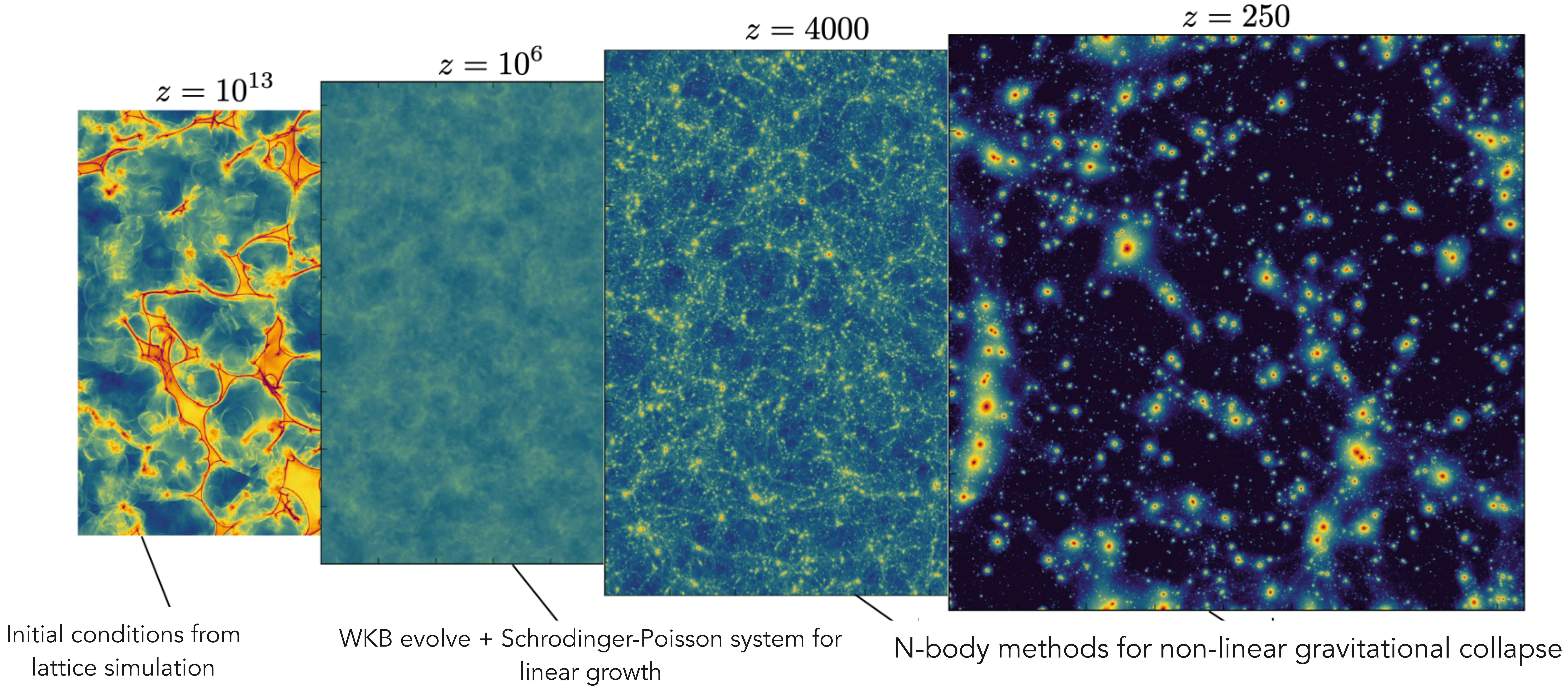

Axion miniclusters are *beyond*-CDM substructure

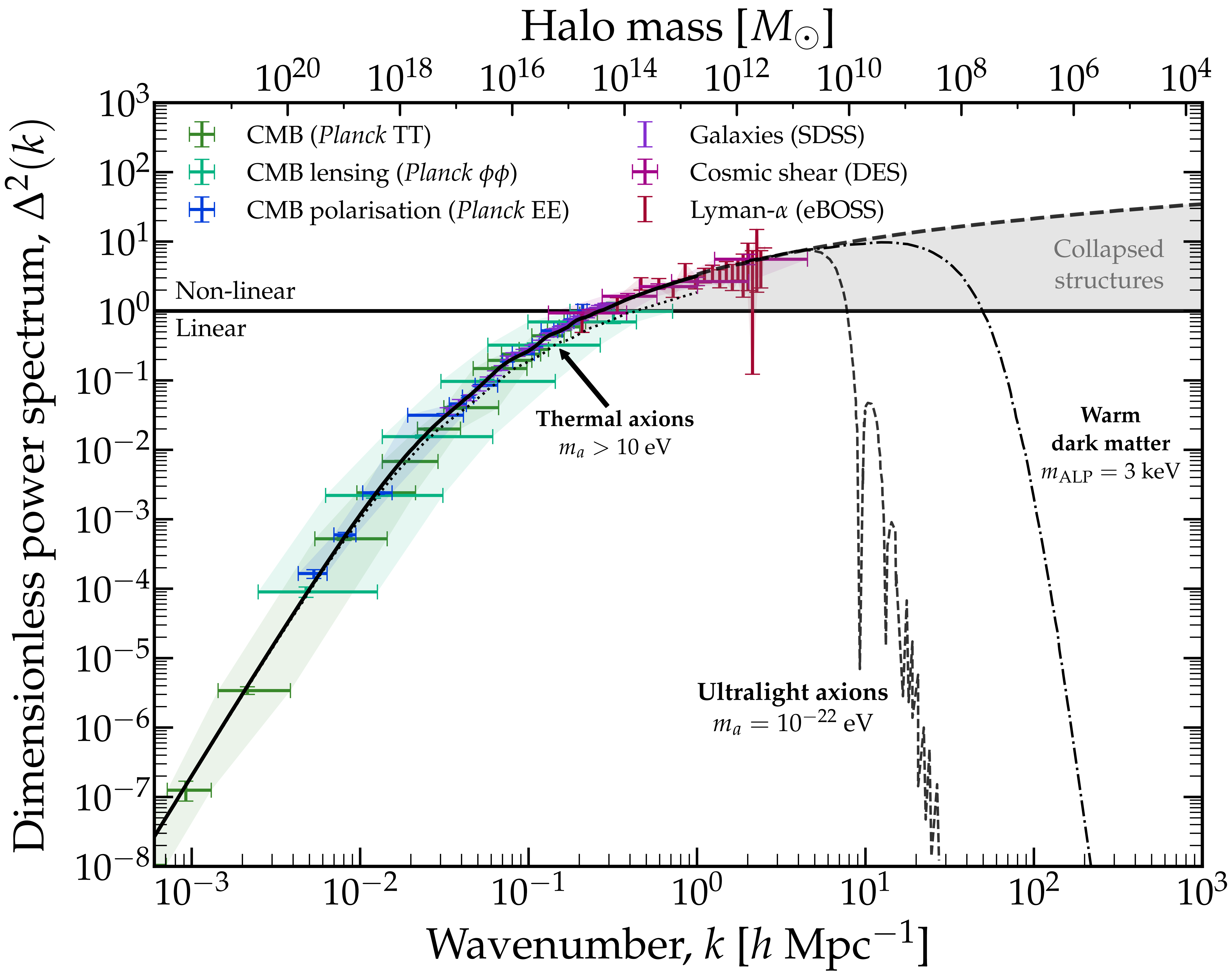

Axion miniclusters are *beyond*-CDM substructure

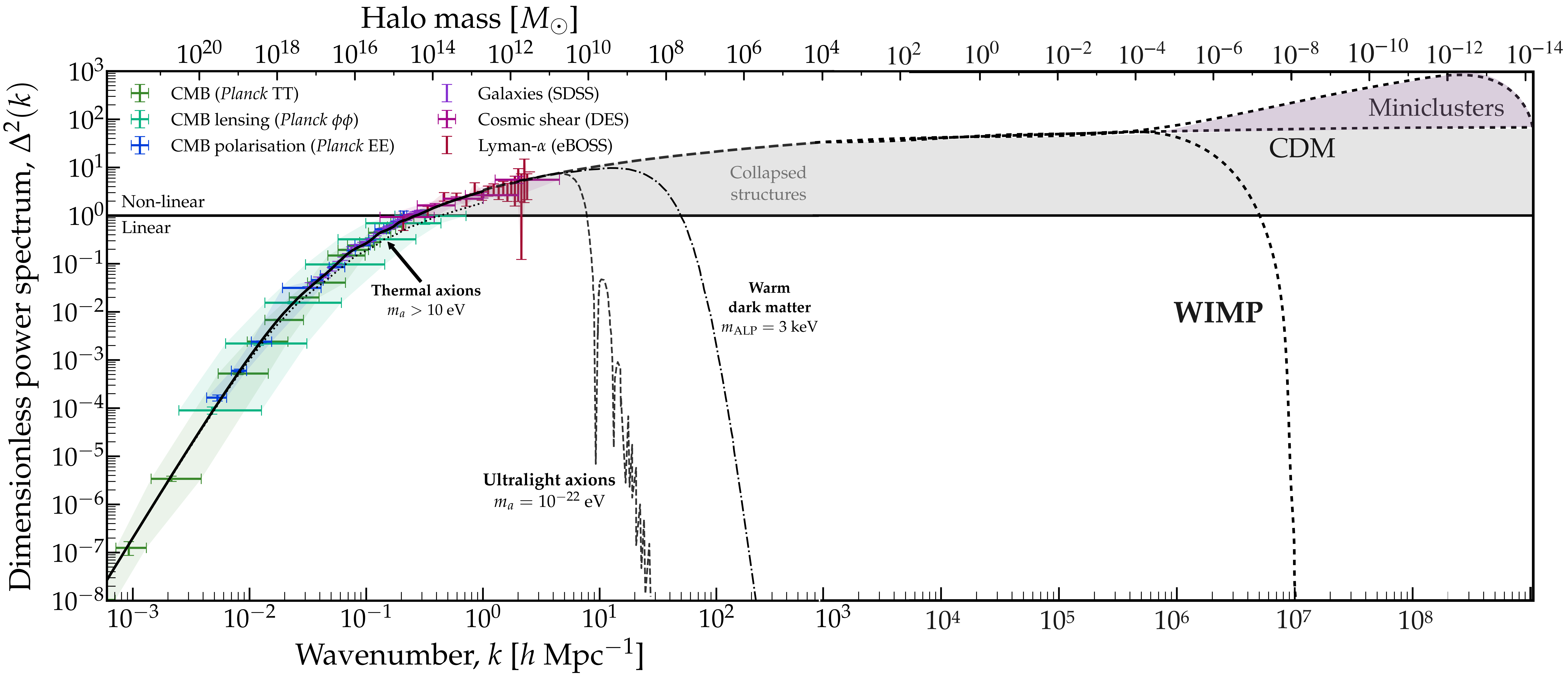

Axion miniclusters

AU—mpc sized gravitationally bound clumps of axions with masses $M \in [10^{-15}, 10^{-9}]\ M_\odot$

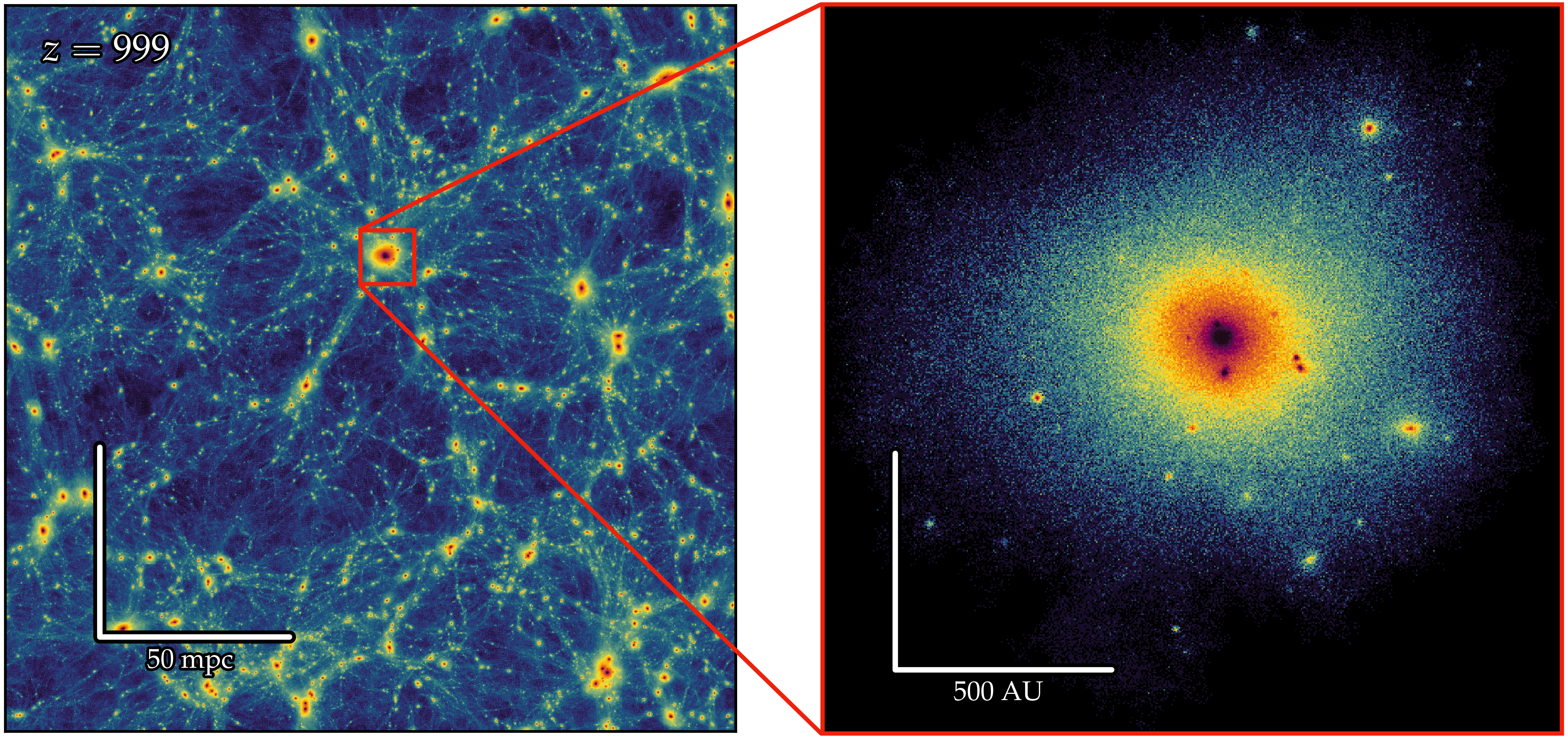

Eggemeier, CAJO+ [2212.00560]

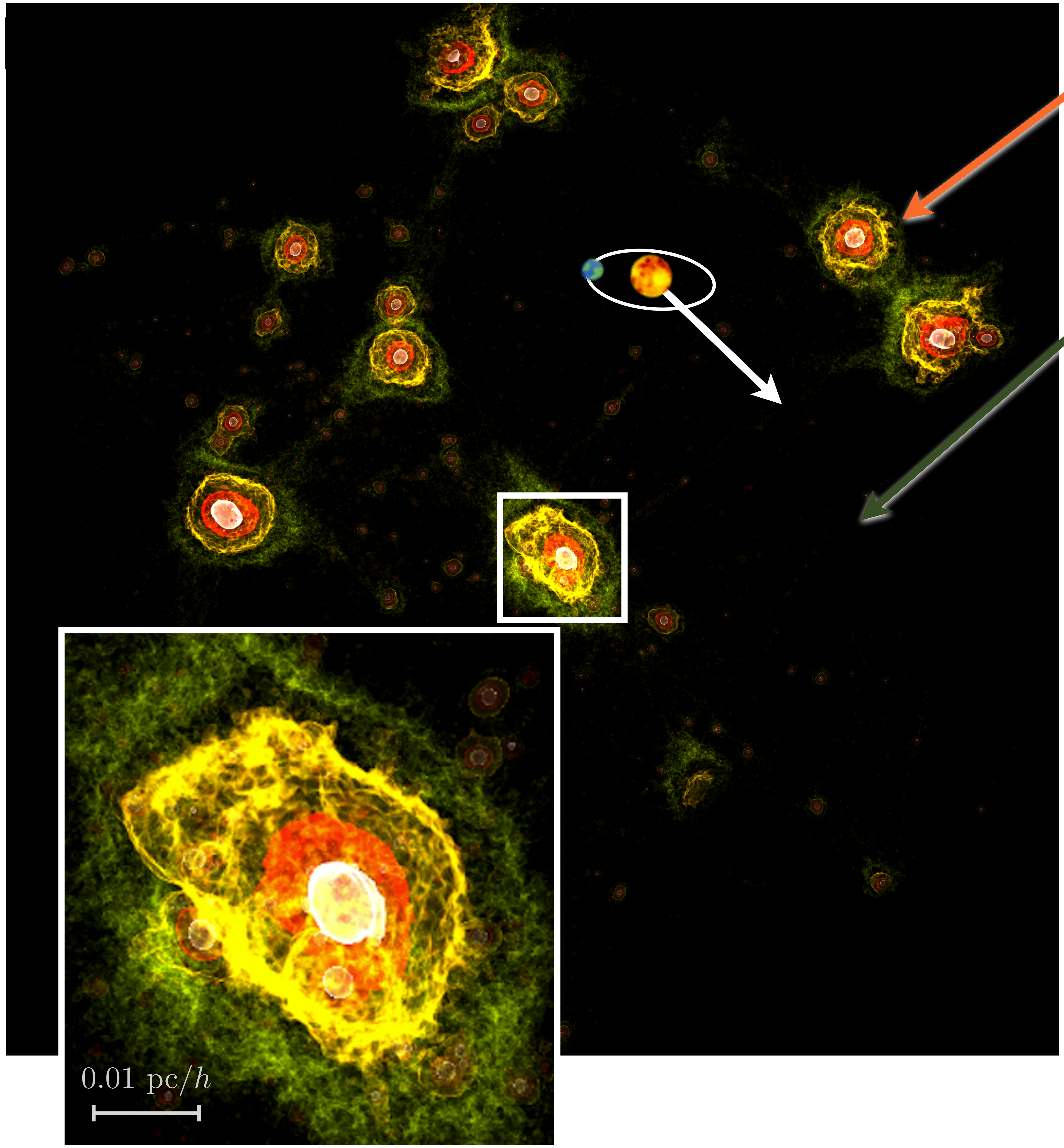

Miniclusters

Minivoids

Miniclusters contain >80% of the axions by mass but make up a tiny (<1%) fraction of the volume.

Earth travels through galaxy at about 0.2 mpc per year, so experiments sample the mini*voids* not the mini*clusters*

This is fairly disastrous for direct detection prospects because accessible DM density is suppressed by up to an order of magnitude

Observational implications

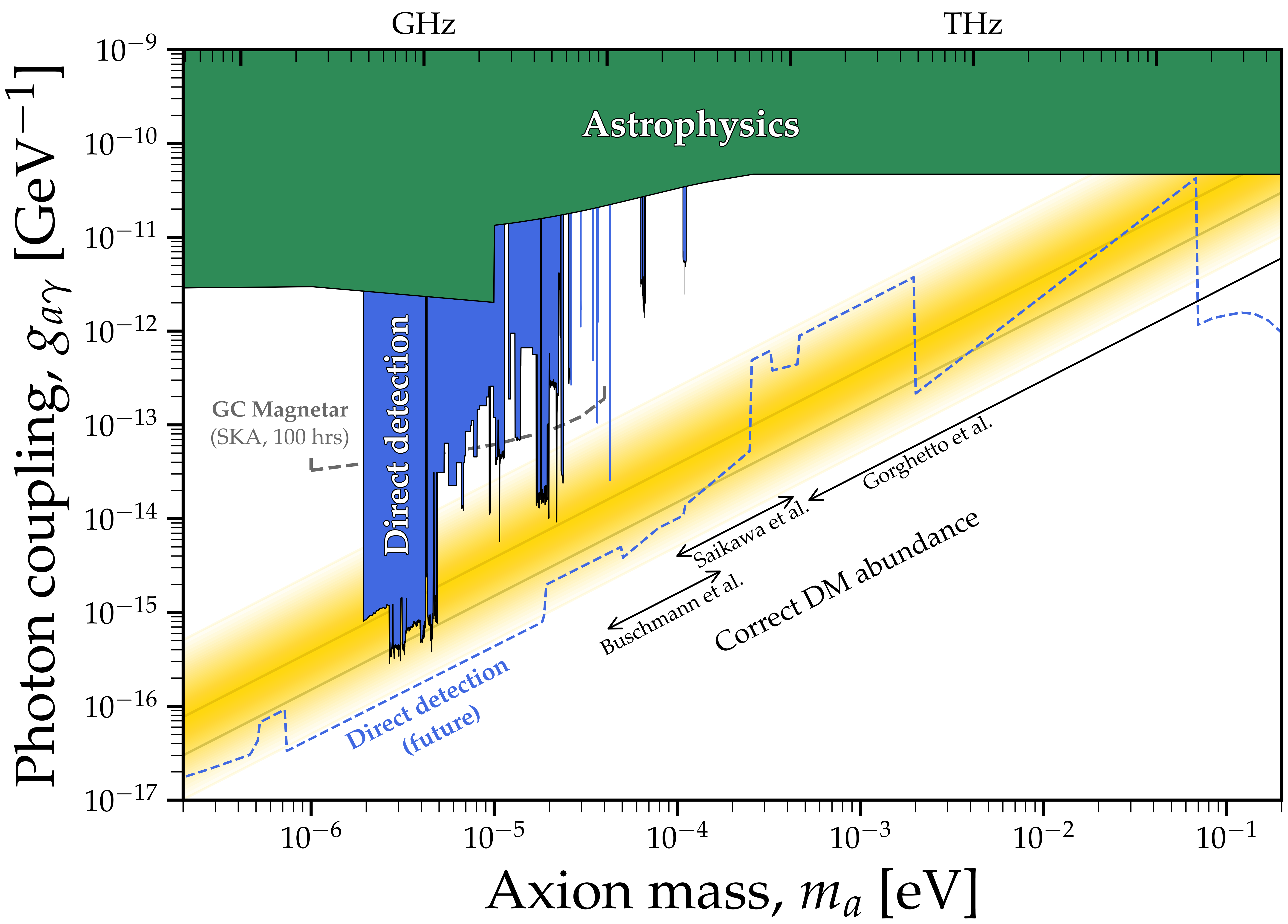

Observational implications

Indirect detection

observe narrow *transient* emission lines at $\omega = m_a$ due to axion miniclusters converting to photons around neutron star magnetospheres

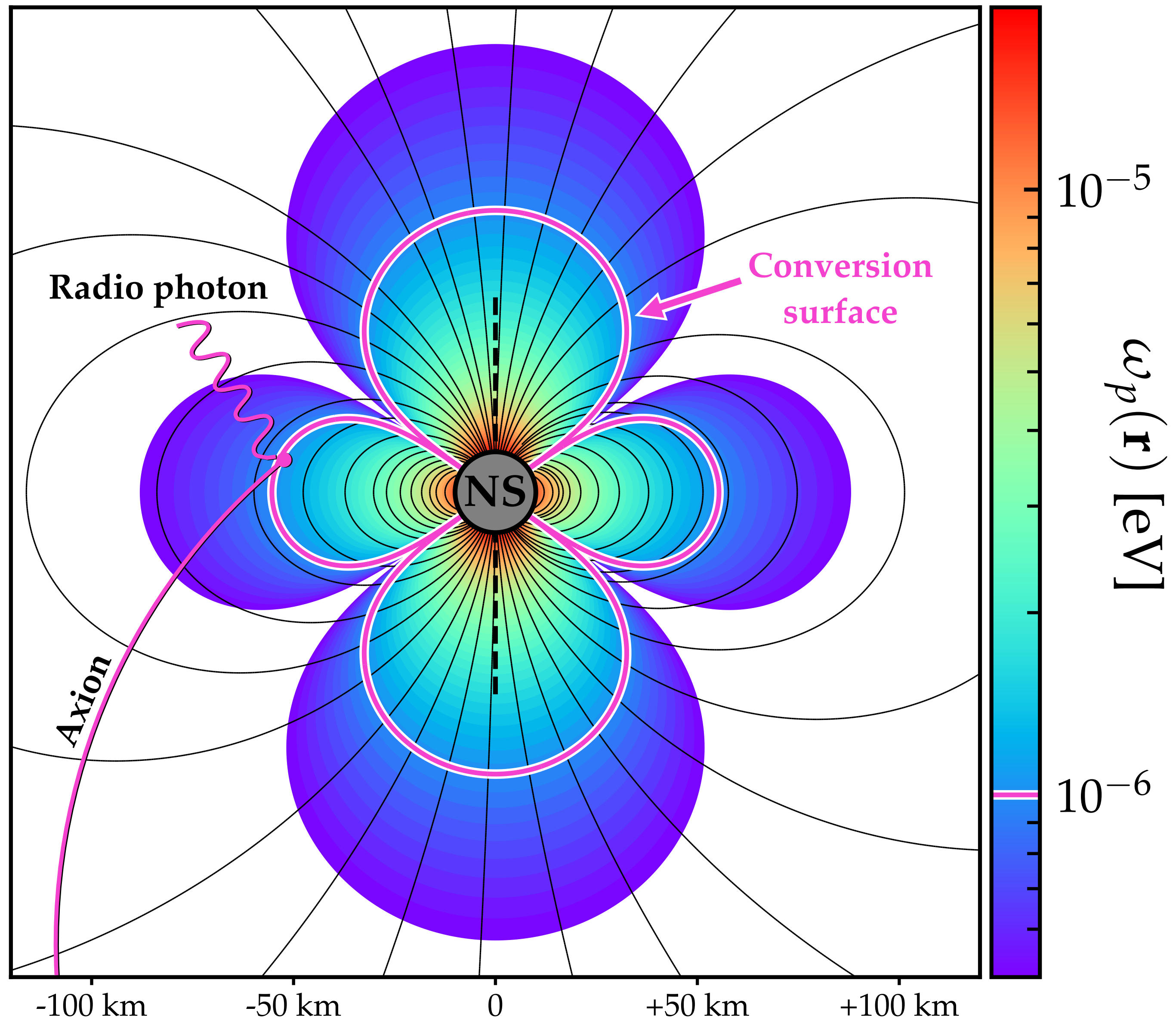

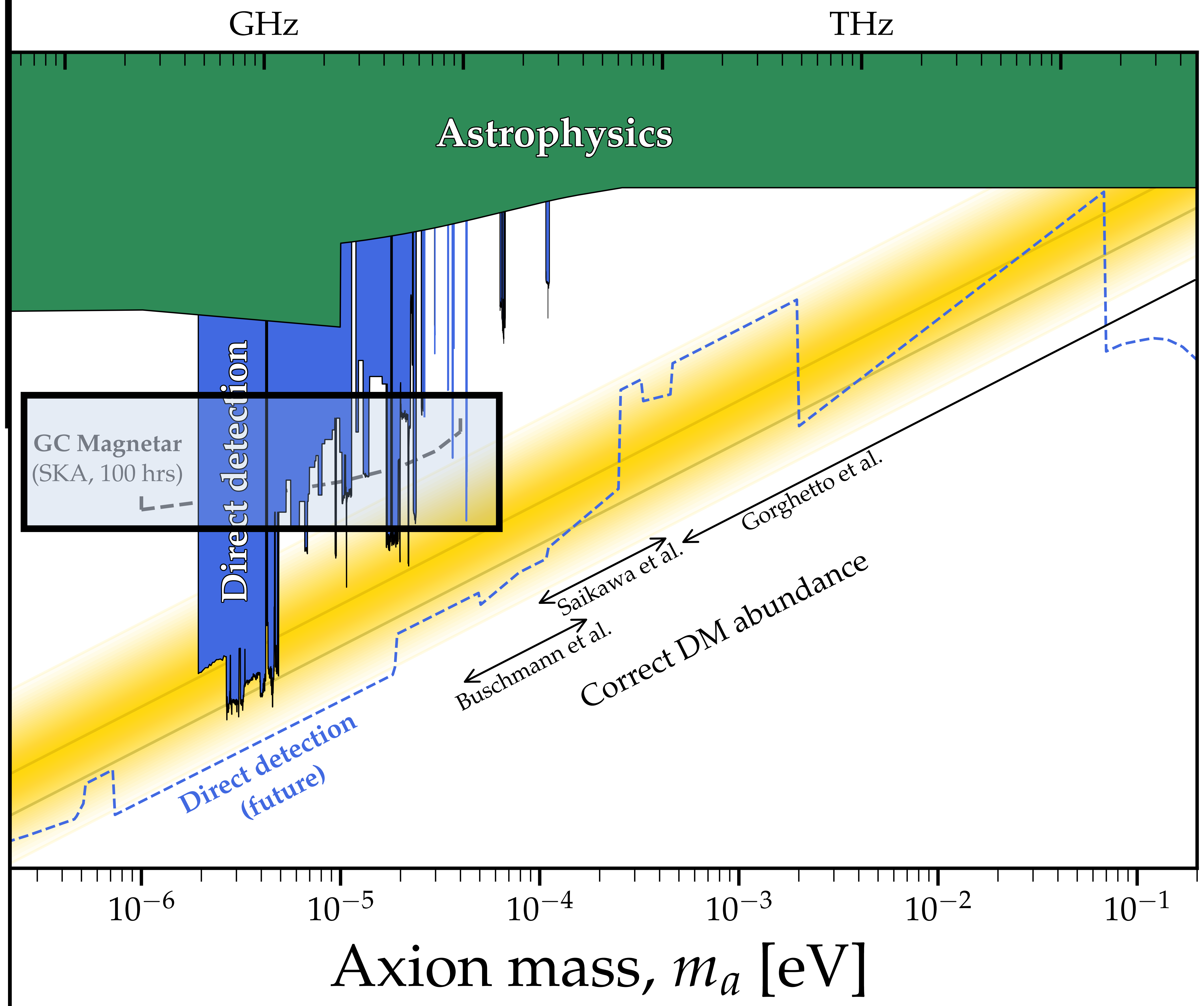

Observational implications

Indirect detection

observe narrow *transient* emission lines at $\omega = m_a$ due to axion miniclusters converting to photons around neutron star magnetospheres

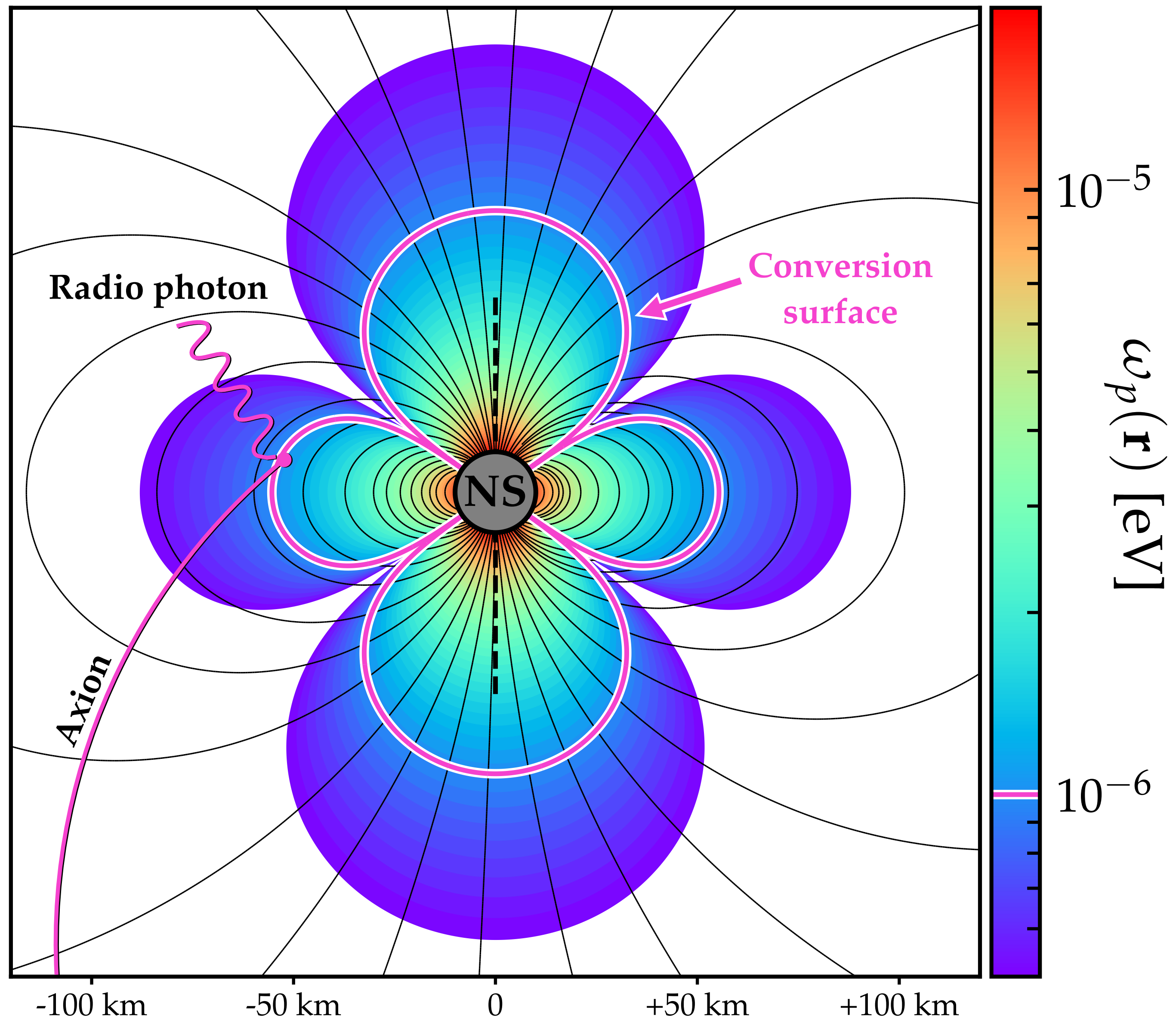

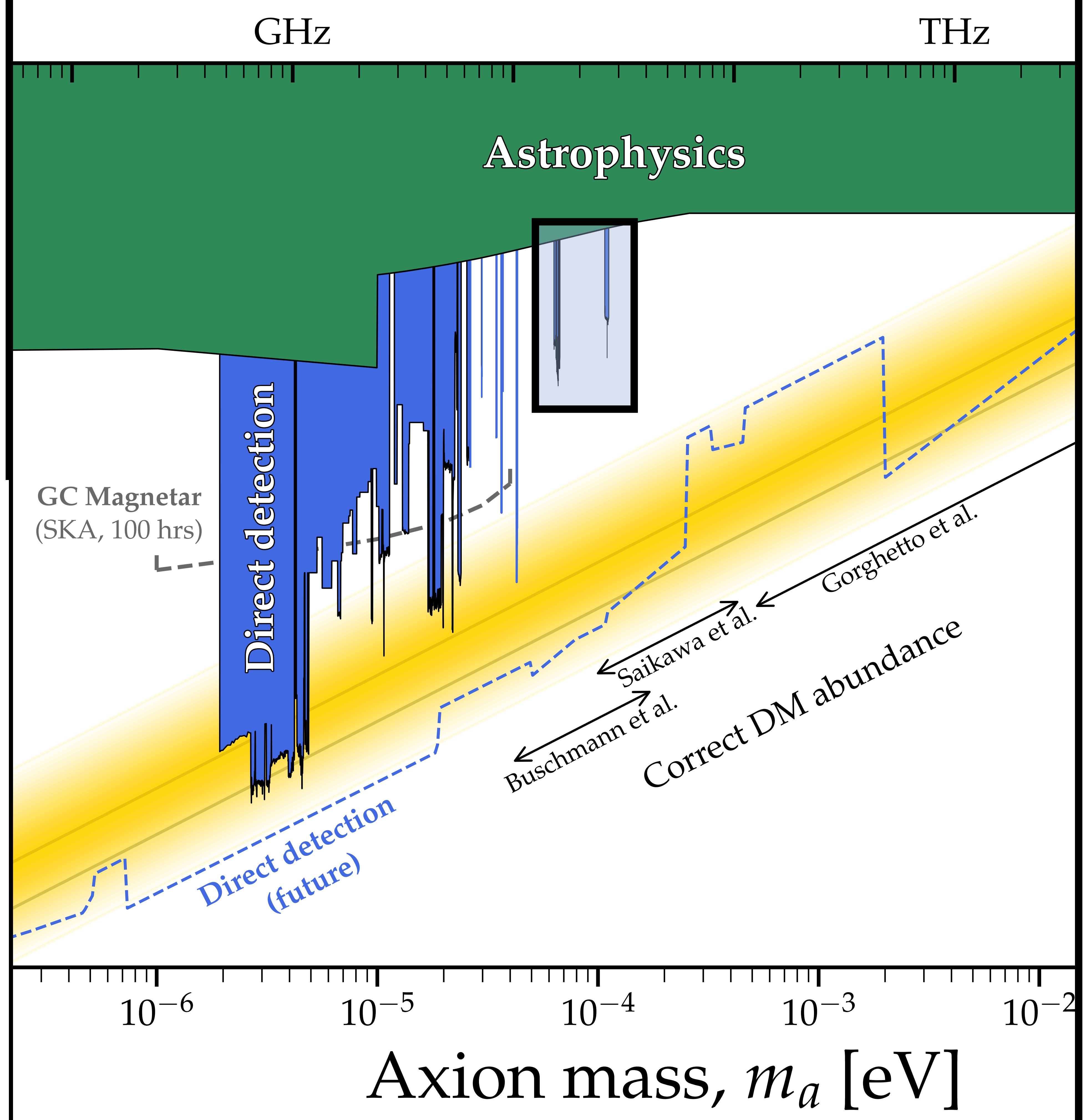

Direct detection

Supression in local density implies suppression in haloscope signal strength. Experiments claiming to reach QCD band, no longer reach QCD band because we live in minivoids.

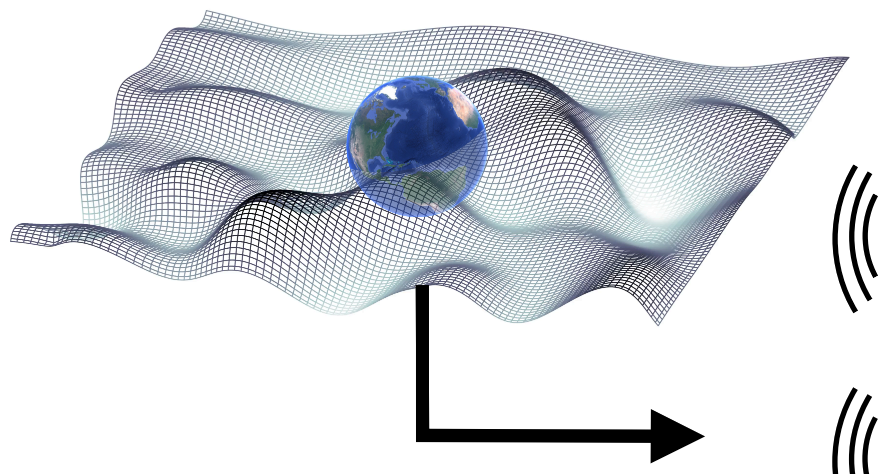

$$|\phi| \propto \sqrt{\rho_{\rm DM}}$$

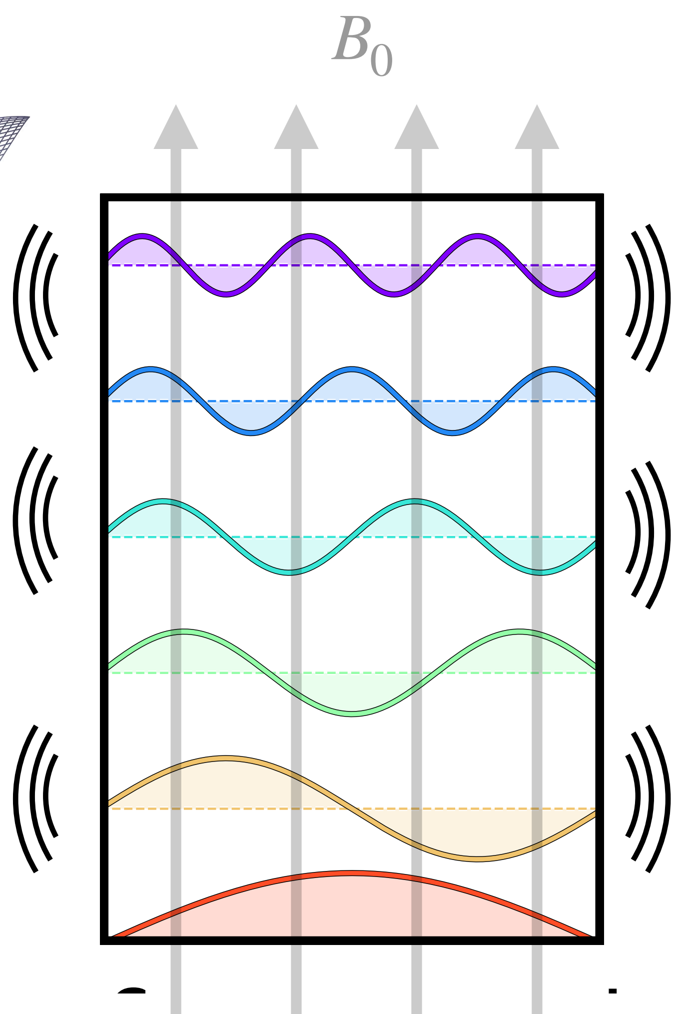

Not the end of the story...

Miniclusters are susceptible to tidal disruption, e.g. when passing stars

$$\Delta E \simeq \left(\frac{2GM_*}{bv_{\rm rel}}\right)^2 \frac{M_{\rm mc}R_{\rm mc}^2}{3}$$

↑

Energy injected into minicluster

Axions with E>Binding energy will evaporate away → form **tidal stream**

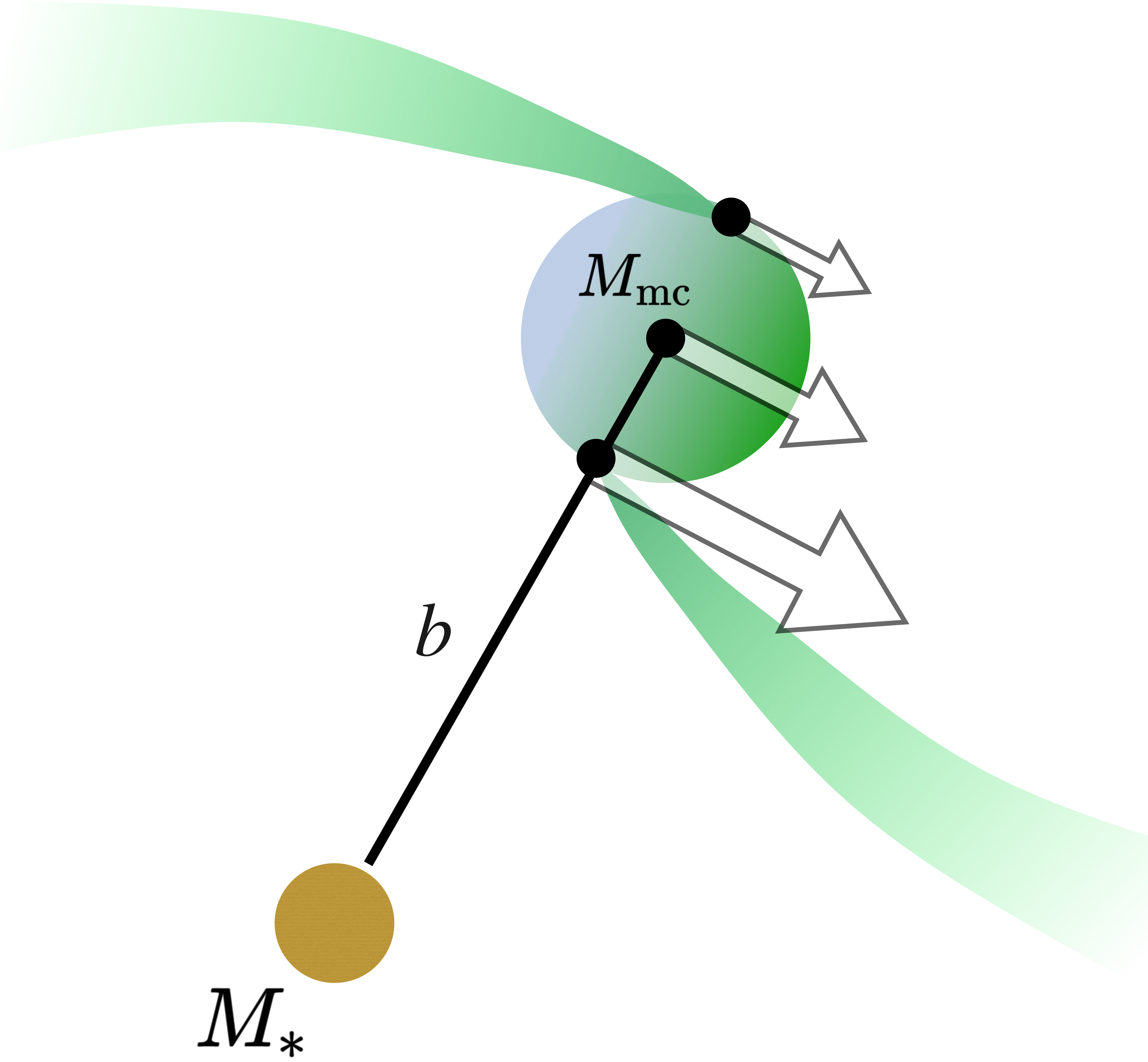

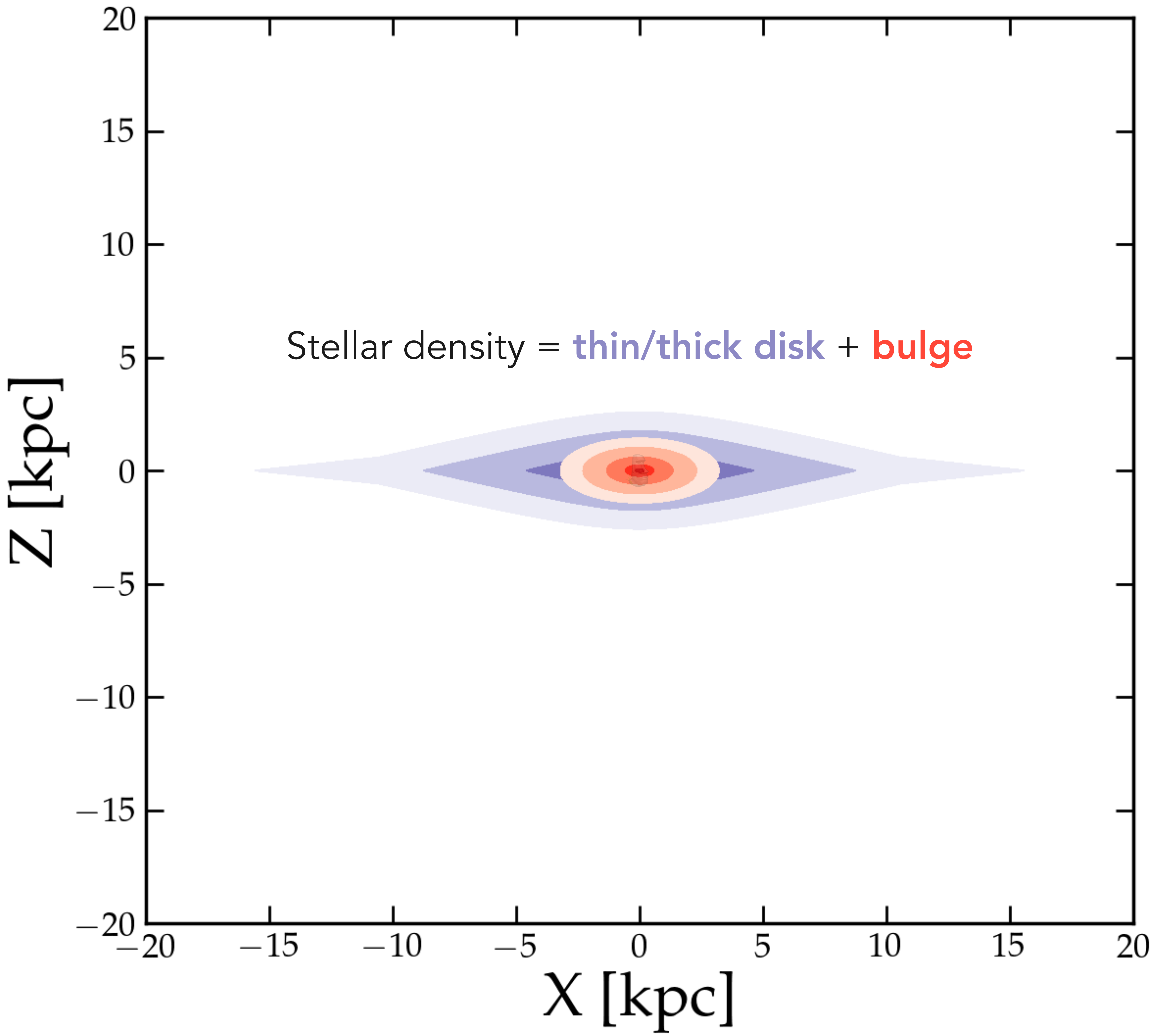

Monte-Carlo simulate miniclusters orbiting the galaxy, undergoing stellar encounters that gradually strip mass away from them

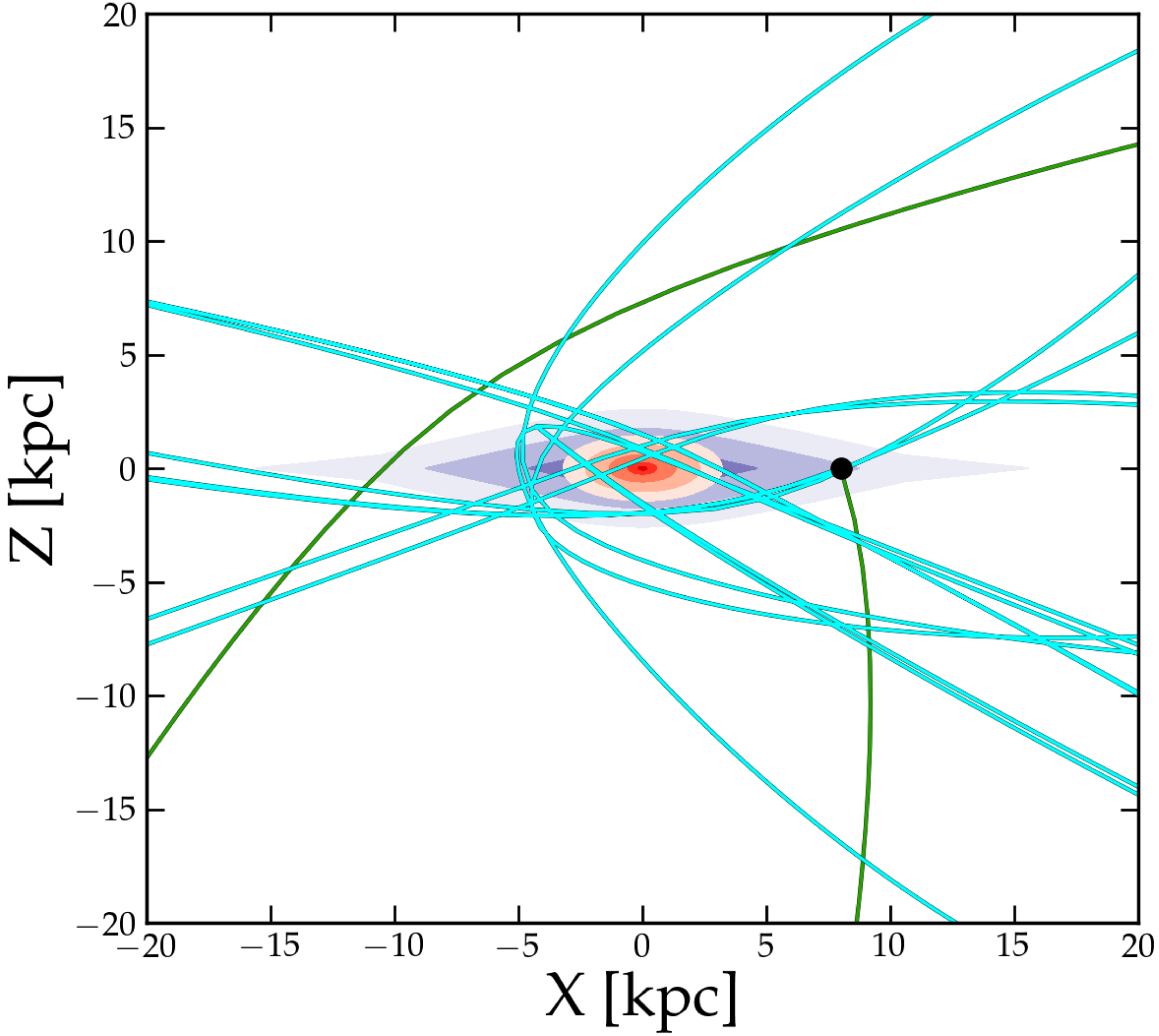

Monte-Carlo simulate miniclusters orbiting the galaxy, undergoing stellar encounters that gradually strip mass away from them

Monte-Carlo simulate miniclusters orbiting the galaxy, undergoing stellar encounters that gradually strip mass away from them

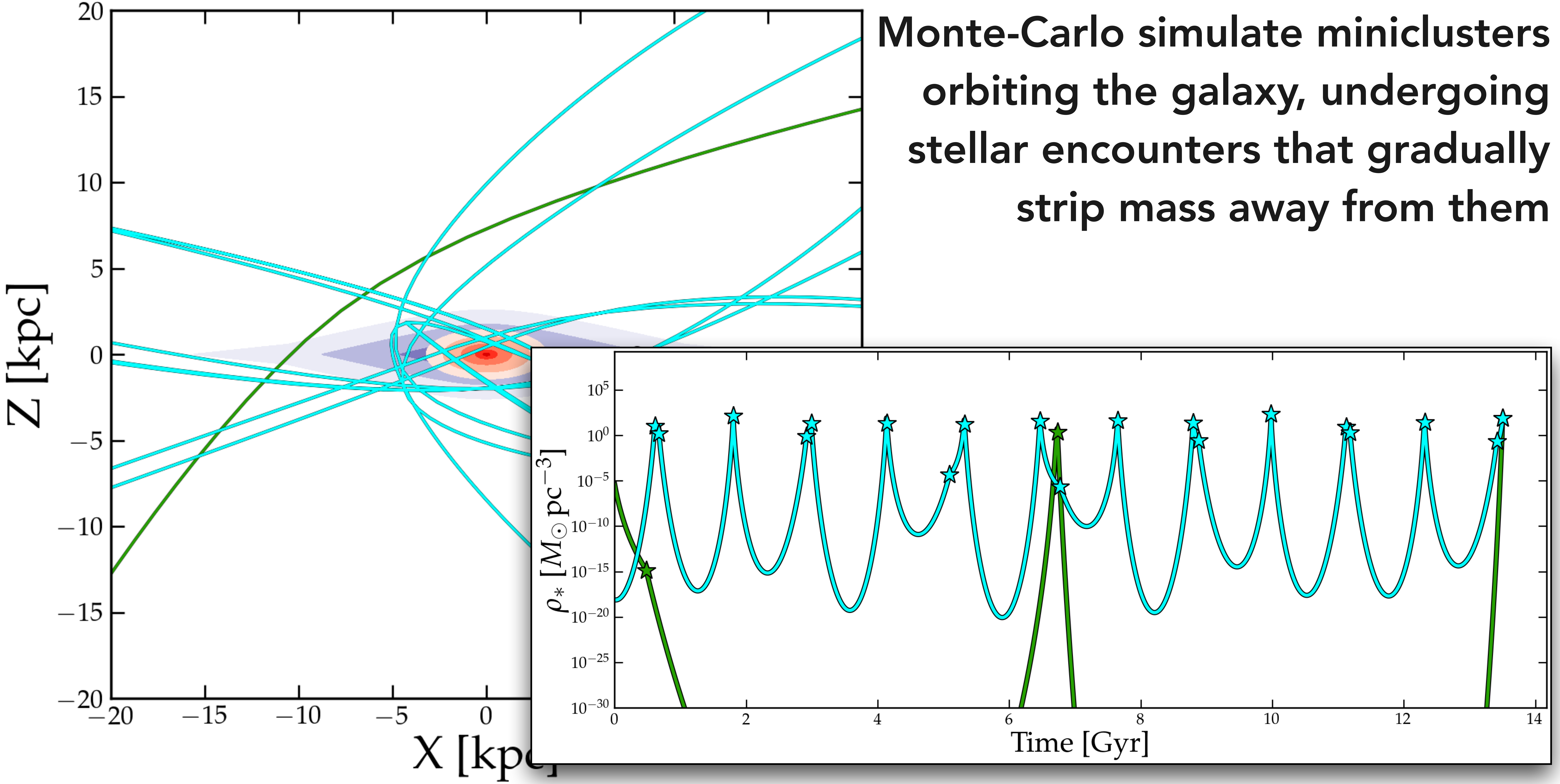

Different populations of miniclusters

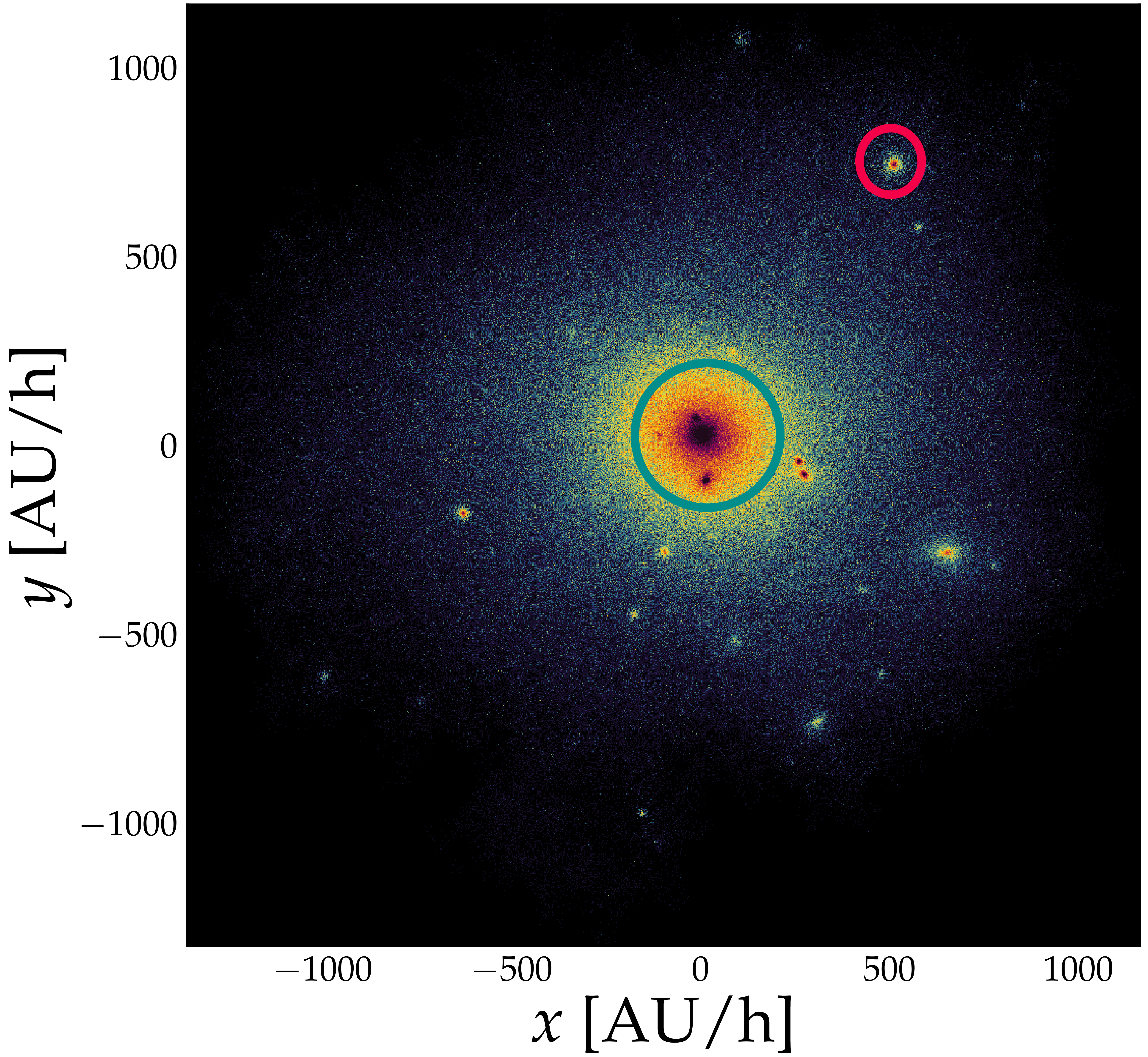

Isolated

- → About 70% of MCs by number
- → Masses $M \in [10^{-16}, 10^{-12}]\, M_{\odot}$
- → Form from prompt collapse of density peaks
- → Power law density profiles $\rho \sim r^{-2.71}$
- → ~0% are *fully* disrupted

Merged

- → About 30% of MCs by number
- → Masses $M \in [10^{-12}, 10^{-7}]\, M_{\odot}$
- → Form from mergers of MCs
- → NFW density profile
- → 45% are *fully* disrupted

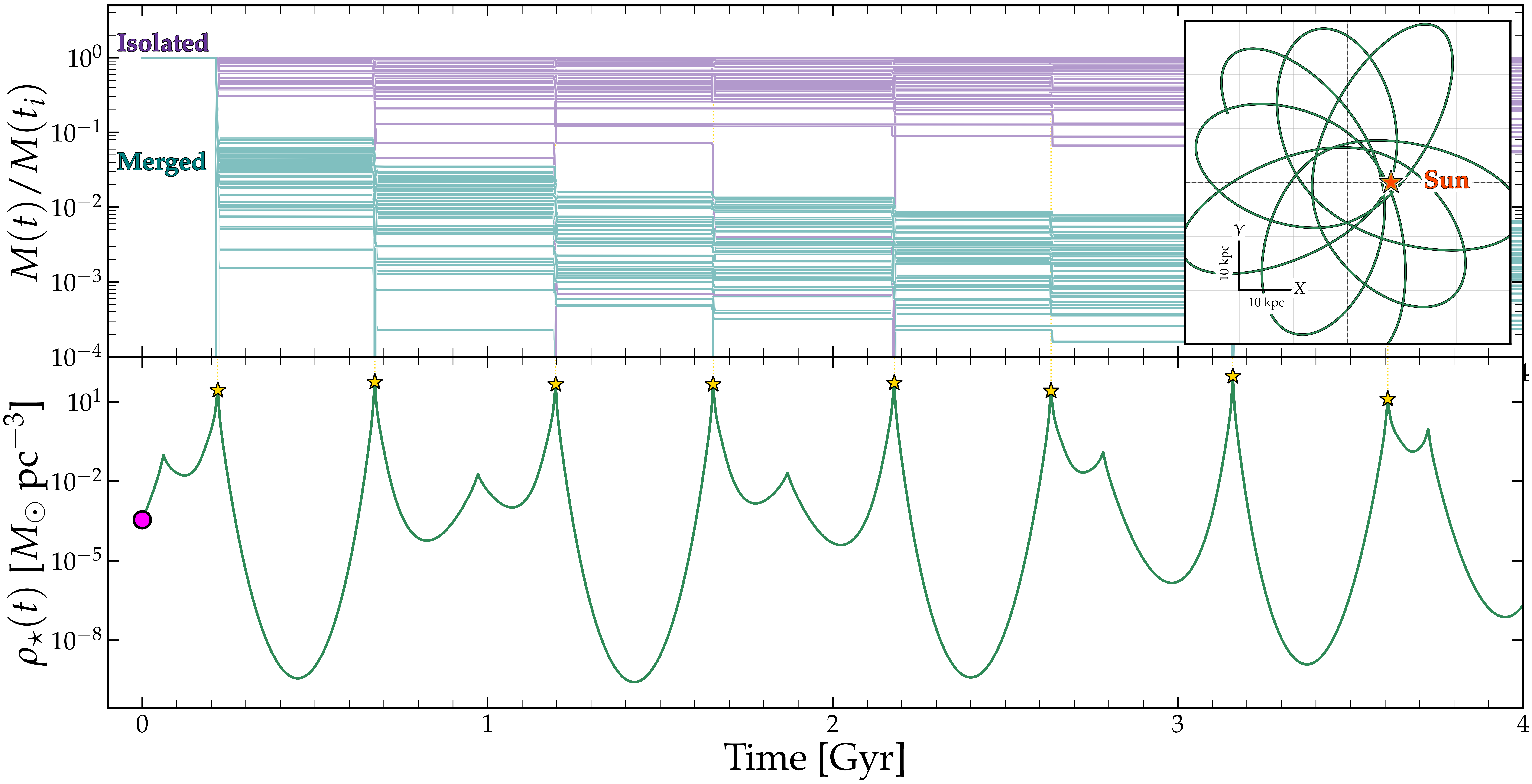

Isolated
Merged
$M(t)/M(t_i)$
10^0
10^{-1}
10^{-2}
10^{-3}
10^{-4}
Sun
Y
X
10 kpc
10 kpc
$\rho_\star(t)$ [$M_\odot$ pc^{-3}]
10^1
10^{-2}
10^{-5}
10^{-8}
0
1
2
3
4
Time [Gyr]

Tidal stream formation

- Axions that are heated beyond the escape speed of the host minicluster will evaporate away, forming tidal stream which will be O(pc) in length
- By the present day, most miniclusters are not 100% disrupted, they leave behind dense cores. However the more massive the minicluster is, the more loosely bound their outer layers are, so by mass >90% of the axions are tidally stripped.

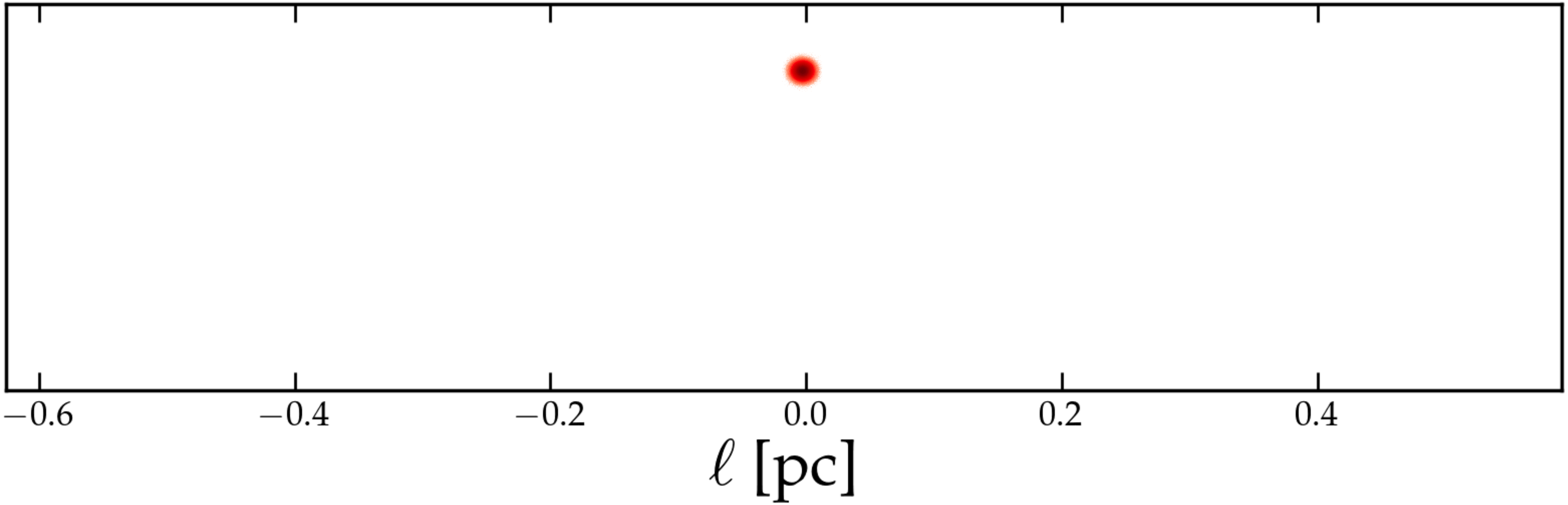

Tidal stream formation

- Axions that are heated beyond the escape speed of the host minicluster will evaporate away, forming tidal stream which will be O(pc) in length
- By the present day, most miniclusters are not 100% disrupted, they leave behind dense cores. However the more massive the minicluster is, the more loosely bound their outer layers are, so by mass >90% of the axions are tidally stripped.

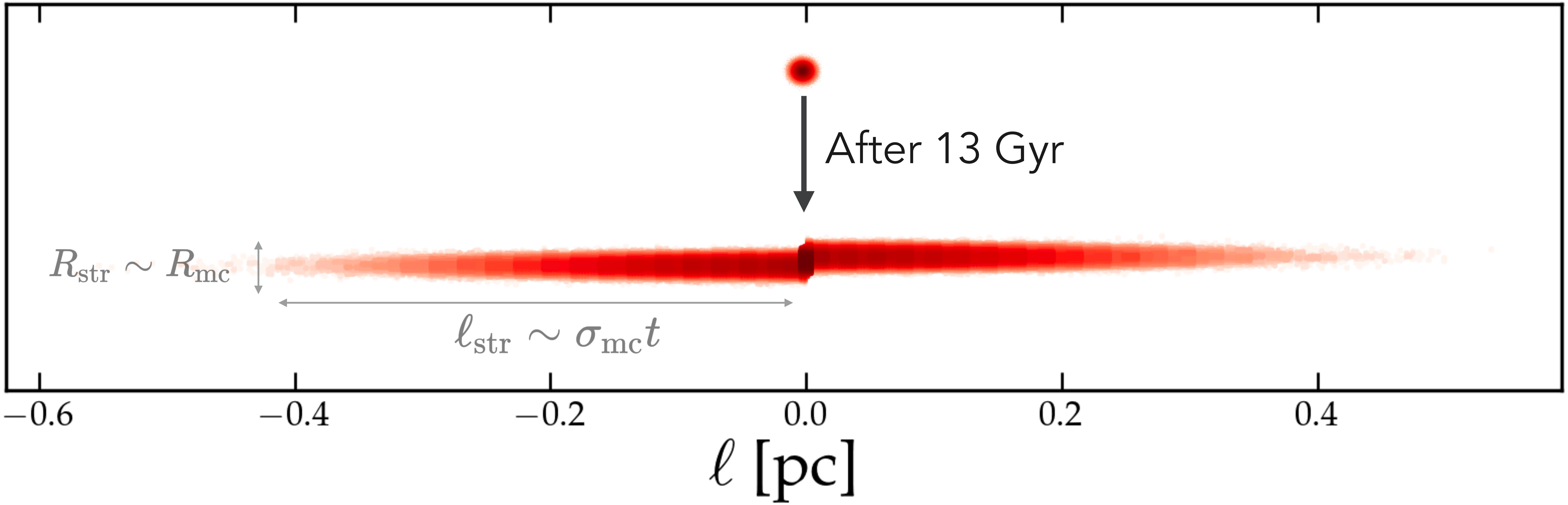

Tidally stripped MCs refill the phase space

We measure $\rho_{\rm DM}$ on scales ~100 pc

→ Must be ~10^{14} miniclusters in that volume

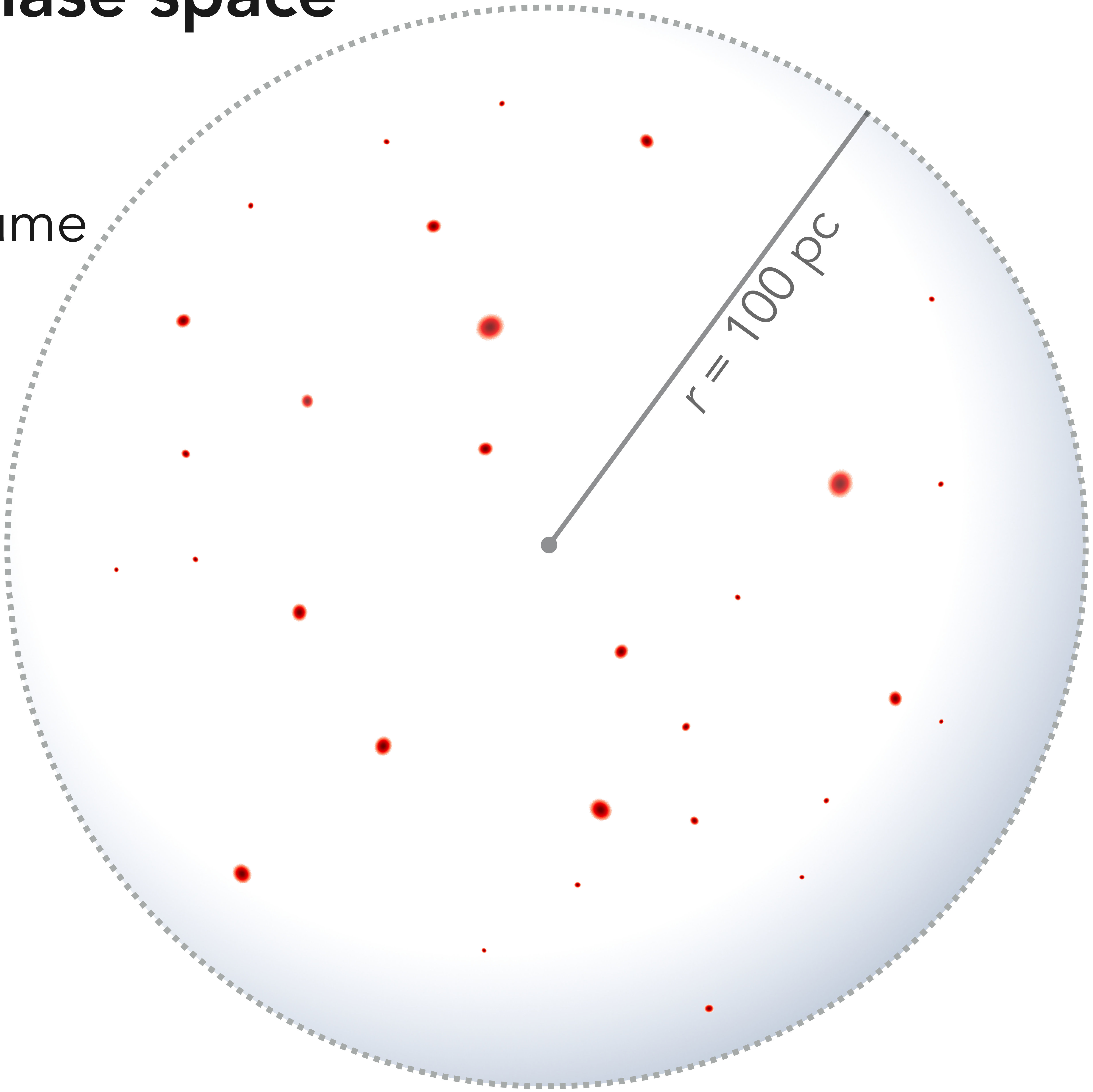

Tidally stripped MCs refill the phase space

We measure $\rho_{\rm DM}$ on scales ~100 pc
→ Must be $\sim 10^{14}$ miniclusters in that volume

After disruption, MCs turn into extended ~pc-long streams. Volume filled with axions is enhanced by a factor of $\sim 10^4$

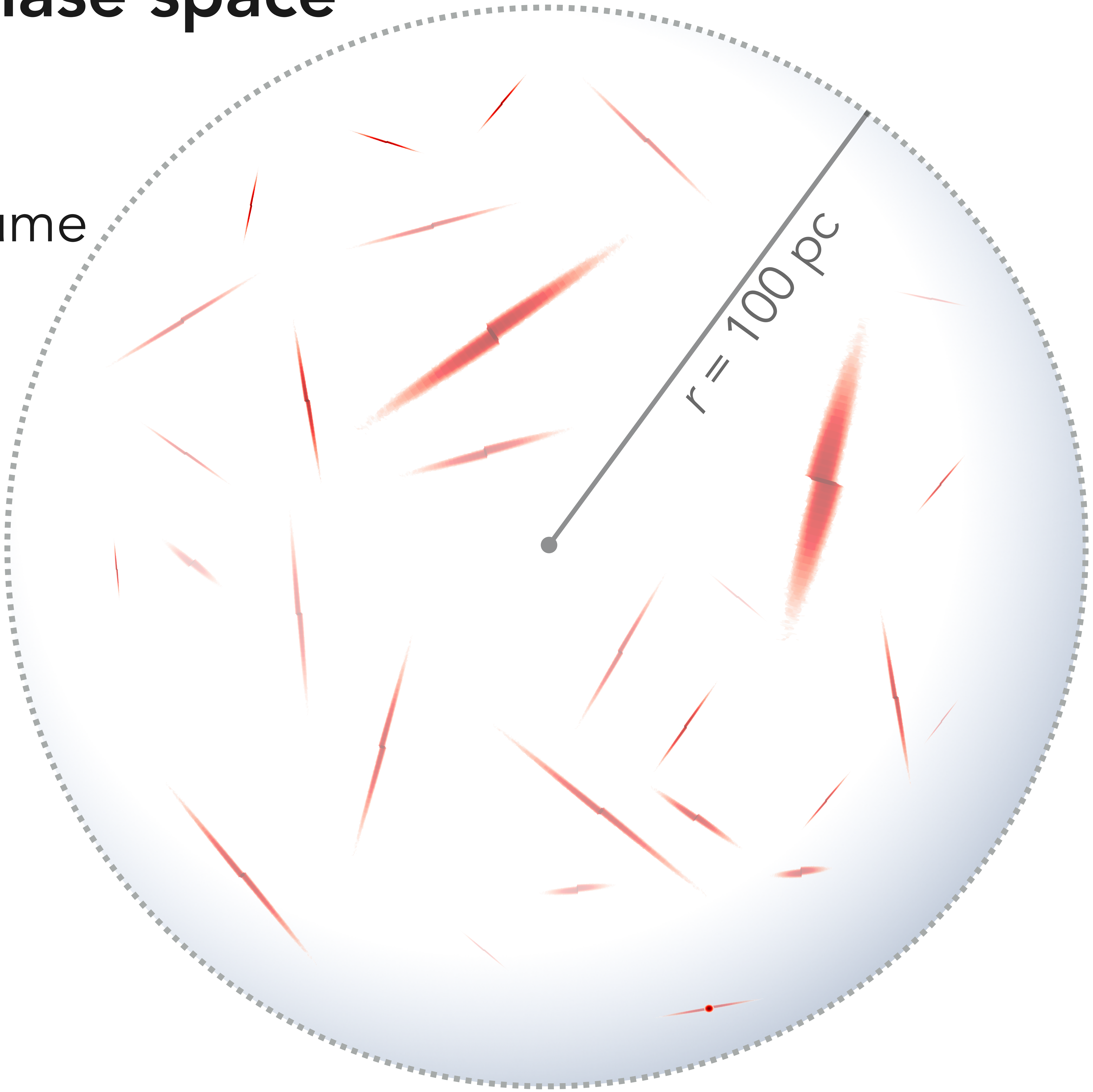

Tidally stripped MCs refill the phase space

We measure ρ_{DM} on scales ~100 pc

→ Must be $\sim 10^{14}$ miniclusters in that volume

After disruption, MCs turn into extended ~pc-long streams. Volume filled with axions is enhanced by a factor of $\sim 10^{4}$

Q: How many streams overlap at a given position in the box?

Q: How much is the density enhanced due to the re-filling of phase space

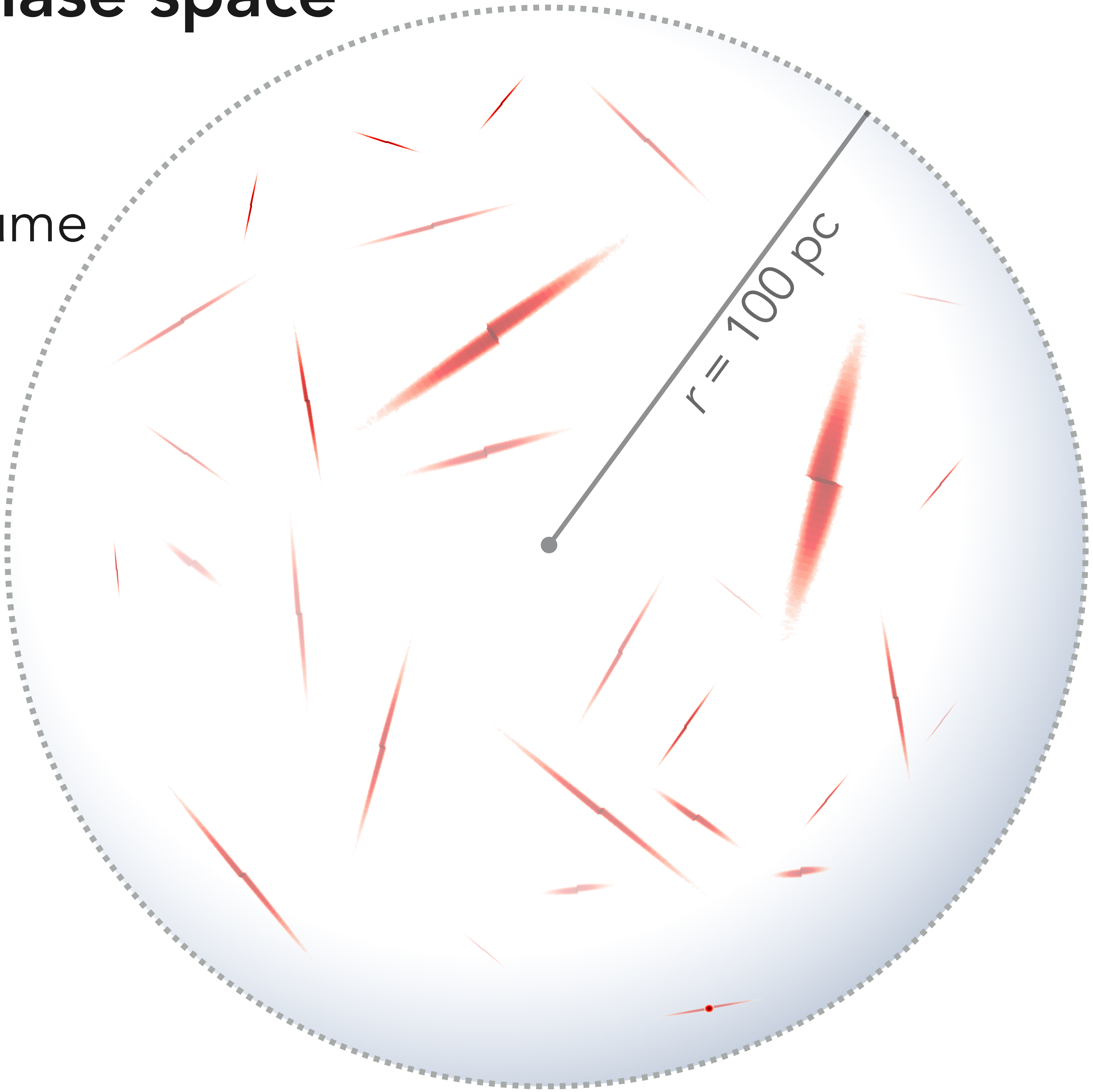

Axion streams at the Solar position

Answer: typically there are O(100-1000) tidal streams overlapping a given position. Vast majority do not contribute substantially to the density

Together they add up to ~70-90% of large-scale measured value of $\rho_{\rm DM}$

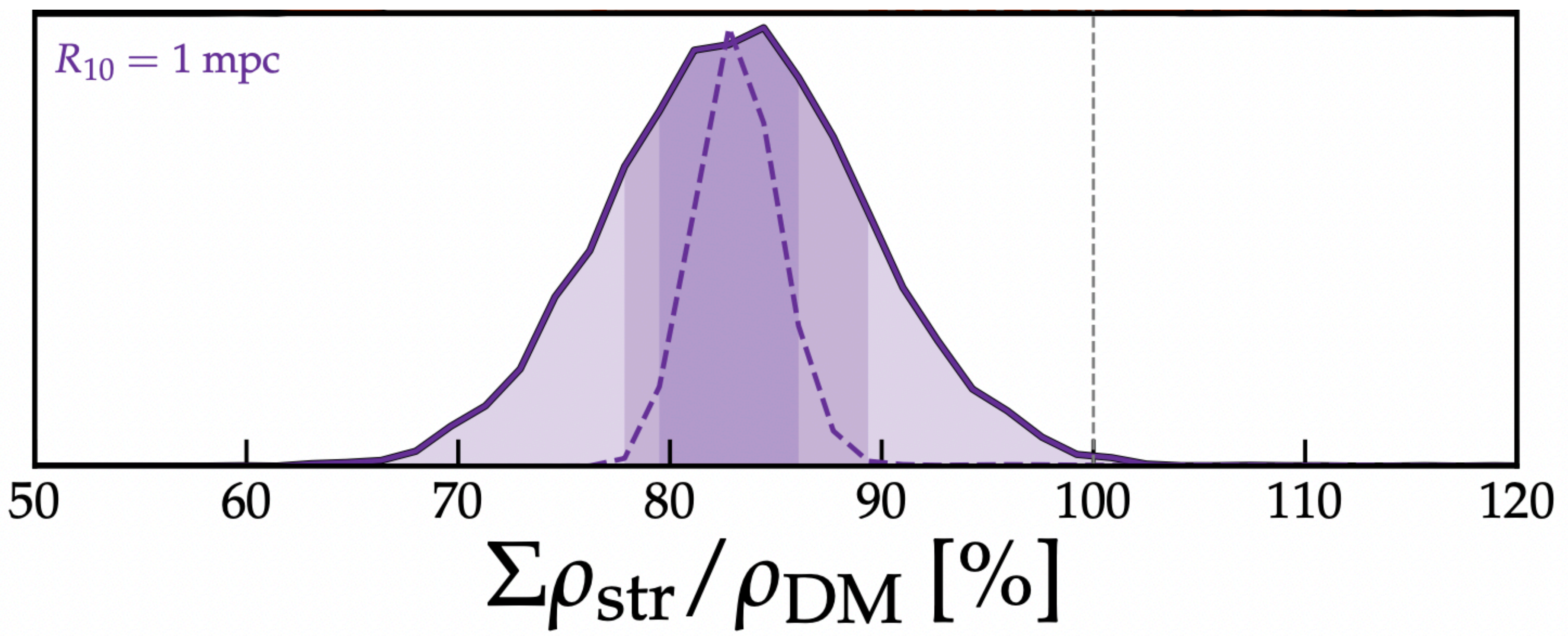

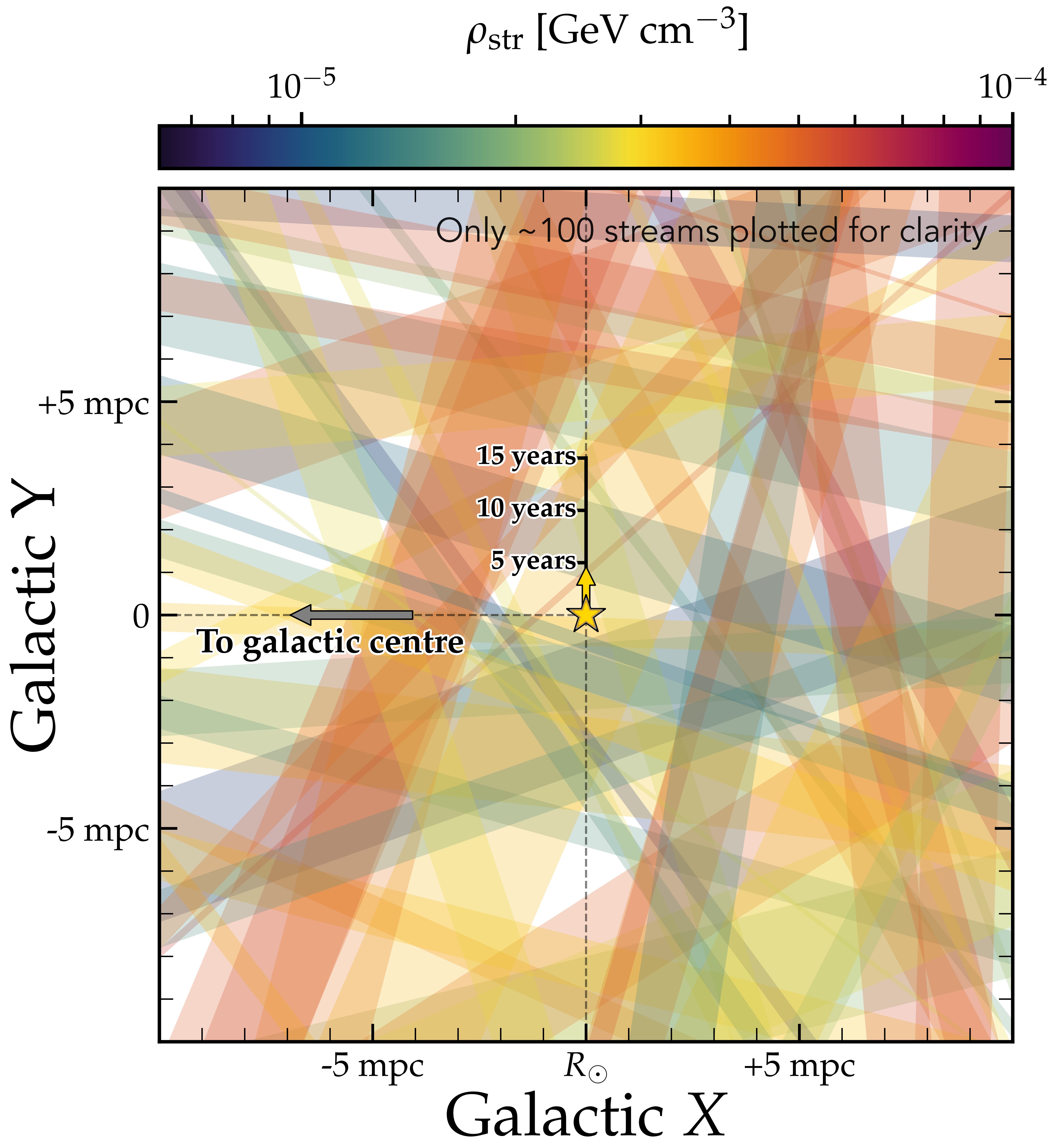

Haloscope signal

The power spectrum of the oscillating axion signal in a haloscope has a distinct Maxwellian **lineshape**. Frequency resolution depends on the duration of the timestream samples that are put through a discrete Fourier transform in order to calculate that power spectrum

$$S(\omega) \propto \frac{\rho_{\rm DM}}{m_a^2} g_{a\gamma}^2 f(\omega)$$

Signal $S(\omega) \propto$ discrete FT of timestream

Frequency resolution = $\Delta\omega \sim T_{\rm int}^{-1}$

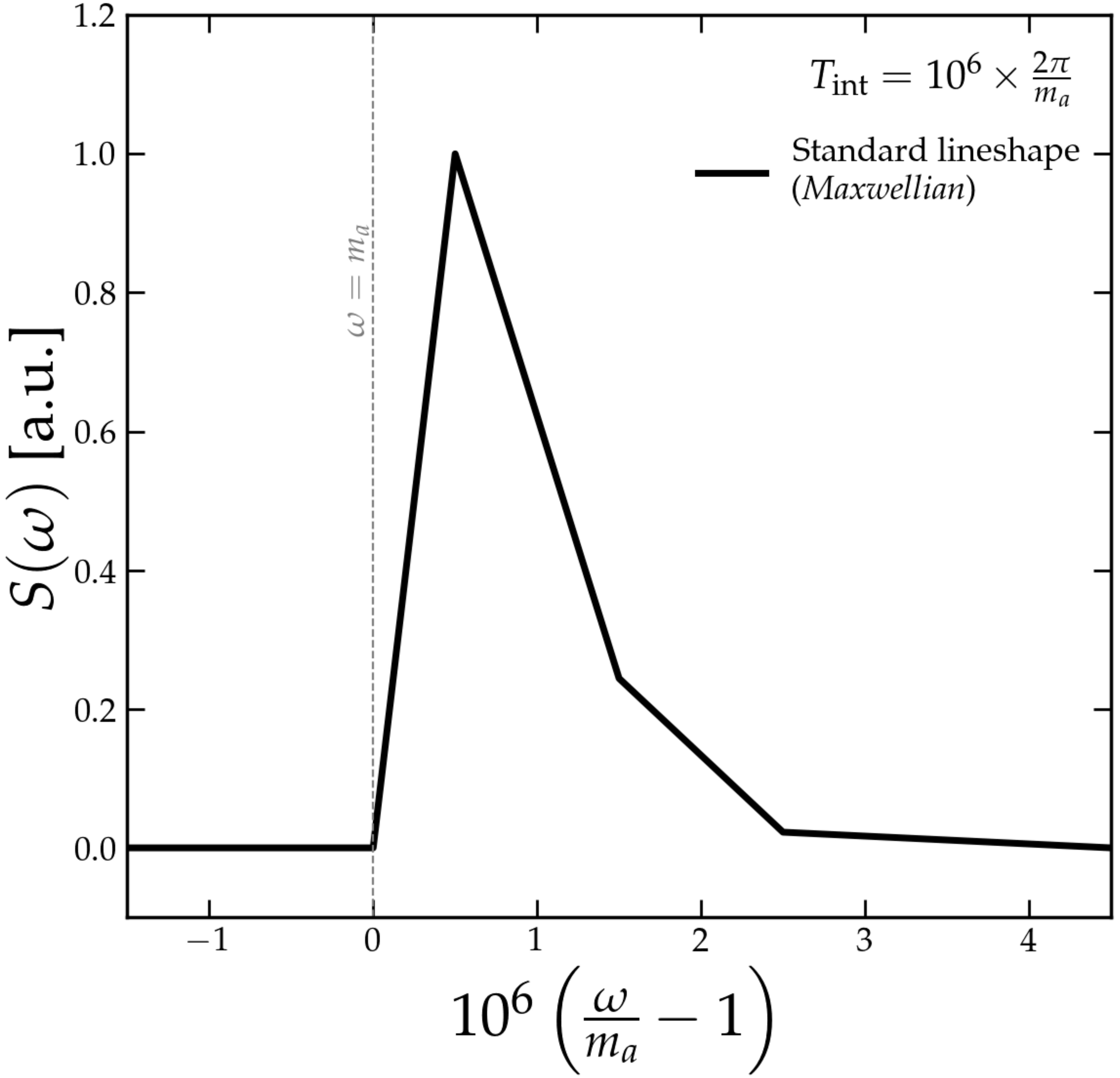

Haloscope signal

The power spectrum of the oscillating axion signal in a haloscope has a distinct Maxwellian **lineshape**. Frequency resolution depends on the duration of the timestream samples that are put through a discrete Fourier transform in order to calculate that power spectrum

$$S(\omega) \propto \frac{\rho_{\rm DM}}{m_a^2} g_{a\gamma}^2 f(\omega)$$

Signal $S(\omega) \propto$ discrete FT of timestream

Frequency resolution = $\Delta\omega \sim T_{\rm int}^{-1}$

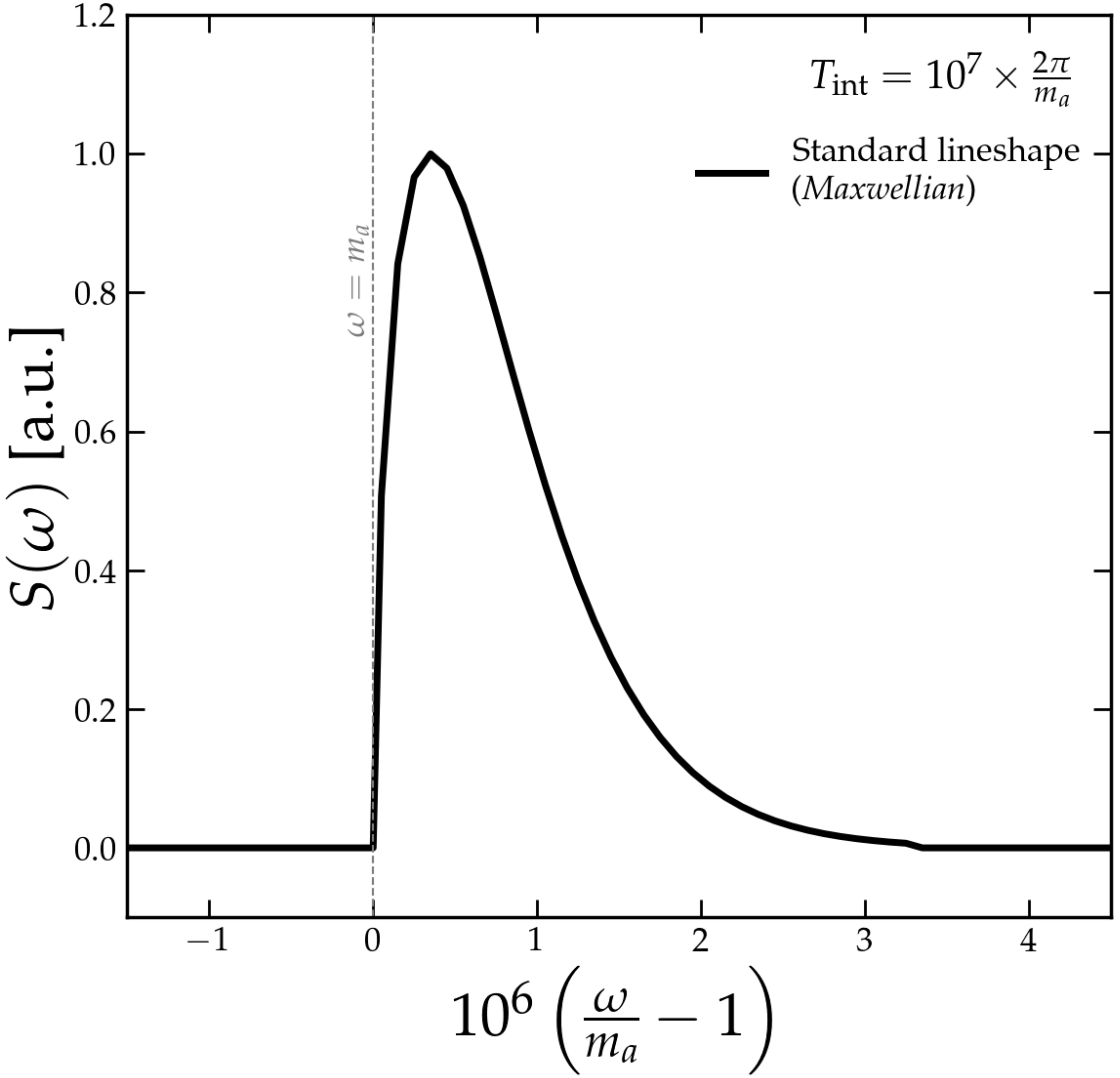

Haloscope signal

The power spectrum of the oscillating axion signal in a haloscope has a distinct Maxwellian **lineshape**. Frequency resolution depends on the duration of the timestream samples that are put through a discrete Fourier transform in order to calculate that power spectrum

$$S(\omega) \propto \frac{\rho_{\mathrm{DM}}}{m_a^2} g_{a\gamma}^2 f(\omega)$$

Signal $S(\omega) \propto$ discrete FT of timestream

Frequency resolution = $\Delta\omega \sim T_{\mathrm{int}}^{-1}$

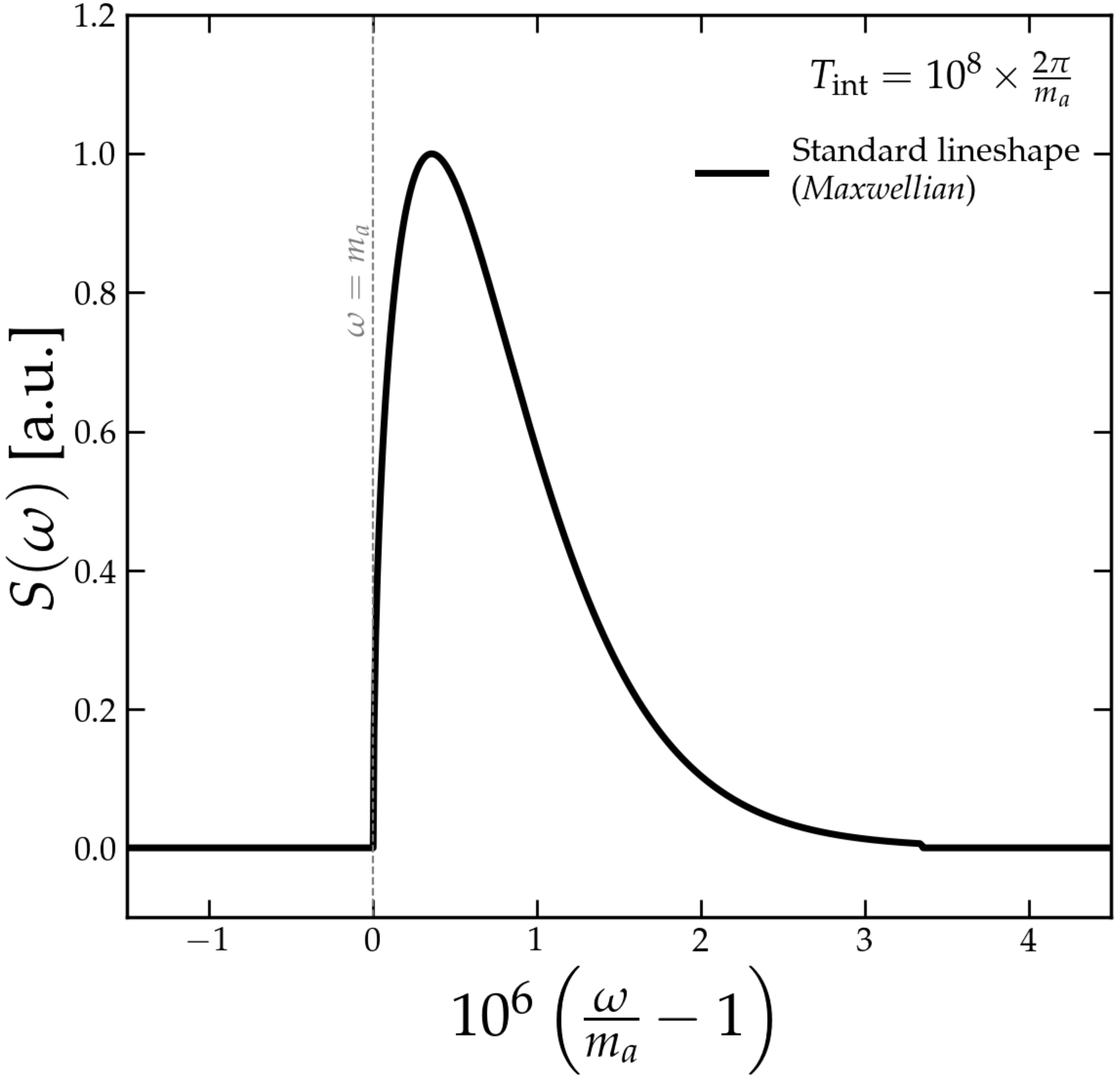

Haloscope signal

The power spectrum of the oscillating axion signal in a haloscope has a distinct Maxwellian **lineshape**. Frequency resolution depends on the duration of the timestream samples that are put through a discrete Fourier transform in order to calculate that power spectrum

$$S(\omega) \propto \frac{\rho_{\rm DM}}{m_a^2} g_{a\gamma}^2 f(\omega)$$

Signal $S(\omega) \propto$ discrete FT of timestream

Frequency resolution = $\Delta\omega \sim T_{\rm int}^{-1}$

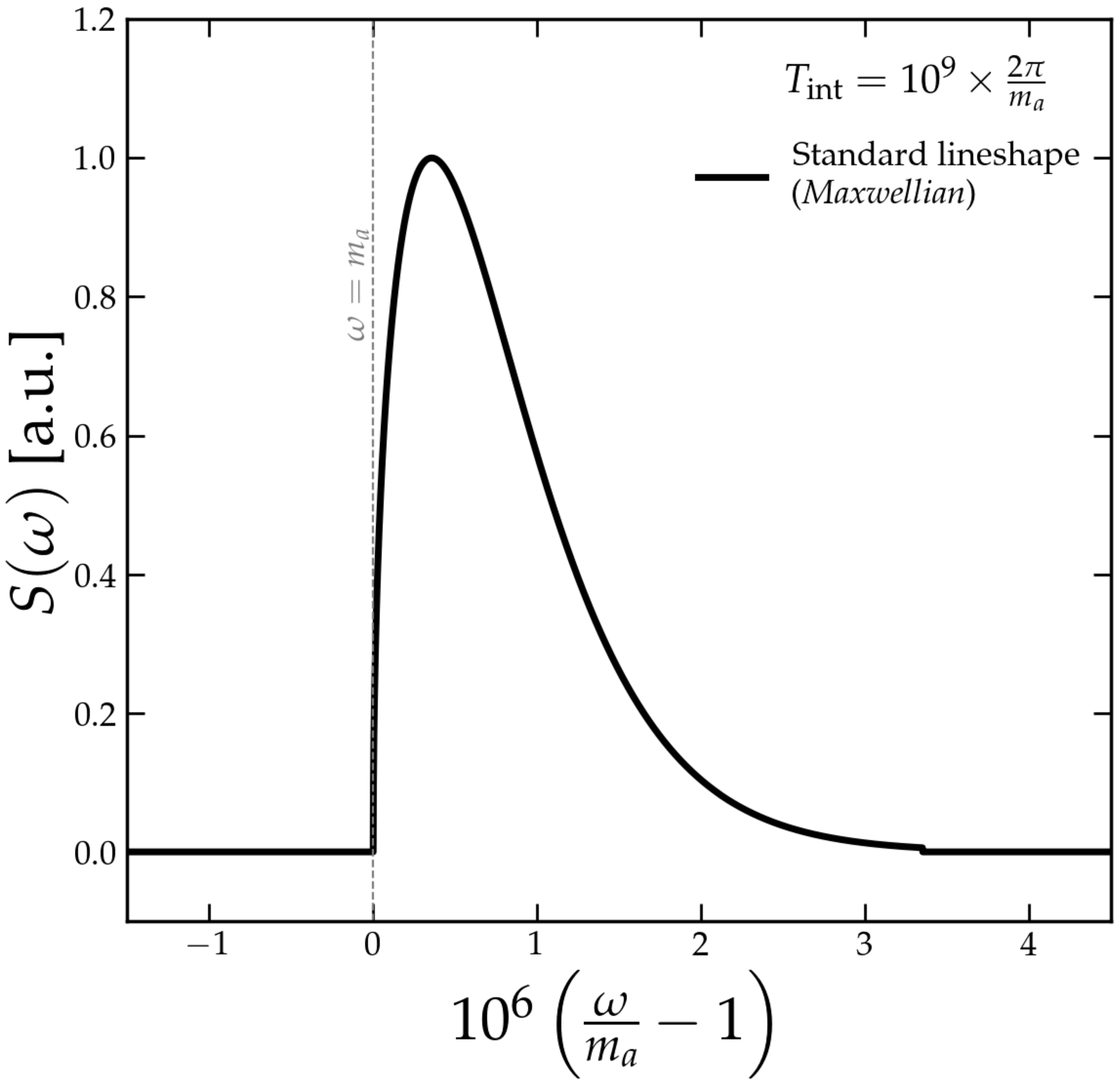

Haloscope signal

Disrupted minicluster **streams** are extremely cold ($\sigma < 1$ km/s) and do not contribute a significant density enhancement. However they become extremely prominent if lineshape is sufficiently well-resolved (long integration times)

Signal $S(\omega) \propto$ discrete FT of timestream

Frequency resolution = $\Delta\omega \sim T_{\rm int}^{-1}$

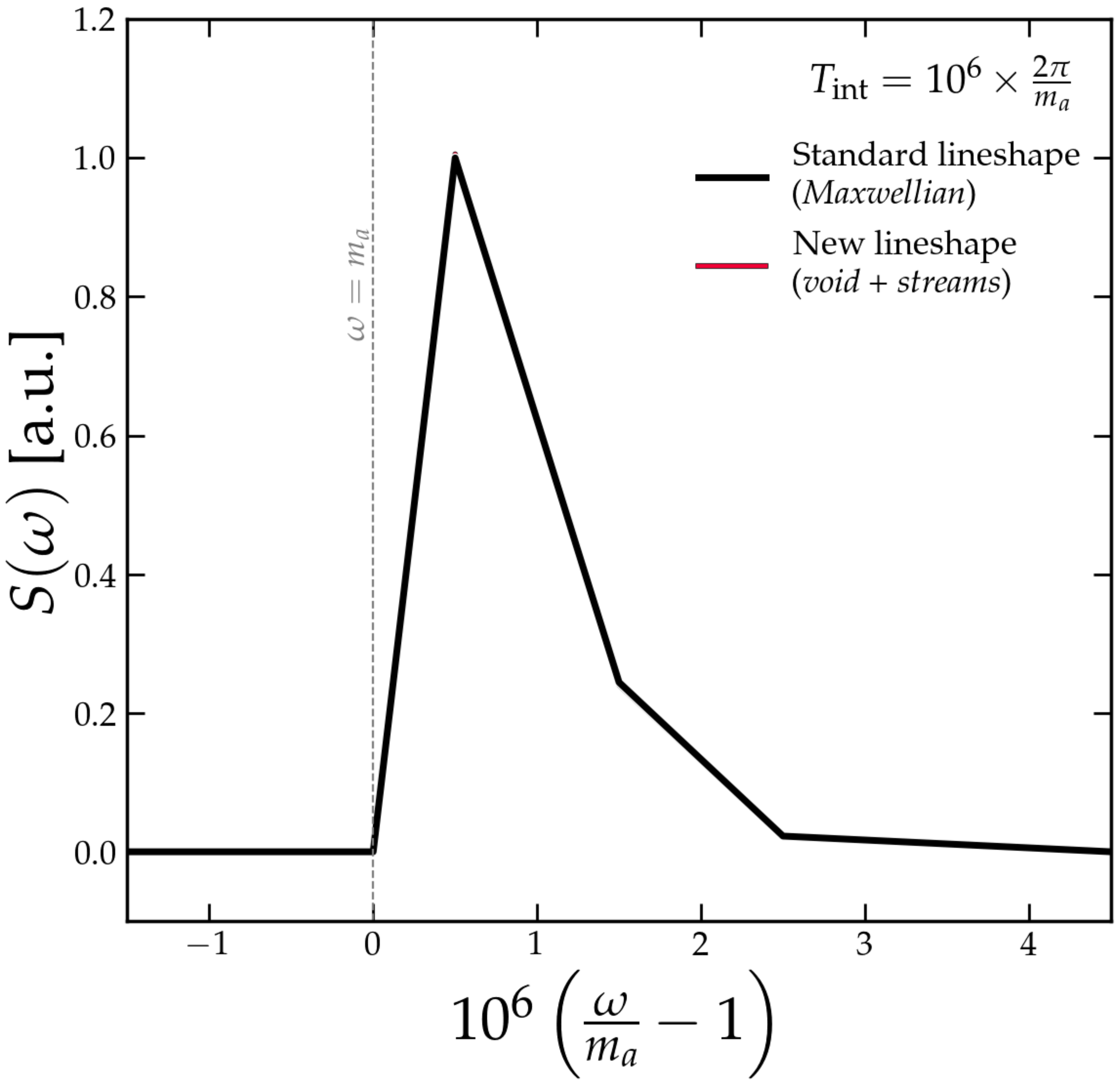

Haloscope signal

Disrupted minicluster **streams** are extremely cold ($\sigma < 1$ km/s) and do not contribute a significant density enhancement. However they become extremely prominent if lineshape is sufficiently well-resolved (long integration times)

Signal $S(\omega) \propto$ discrete FT of timestream

Frequency resolution = $\Delta\omega \sim T_{\rm int}^{-1}$

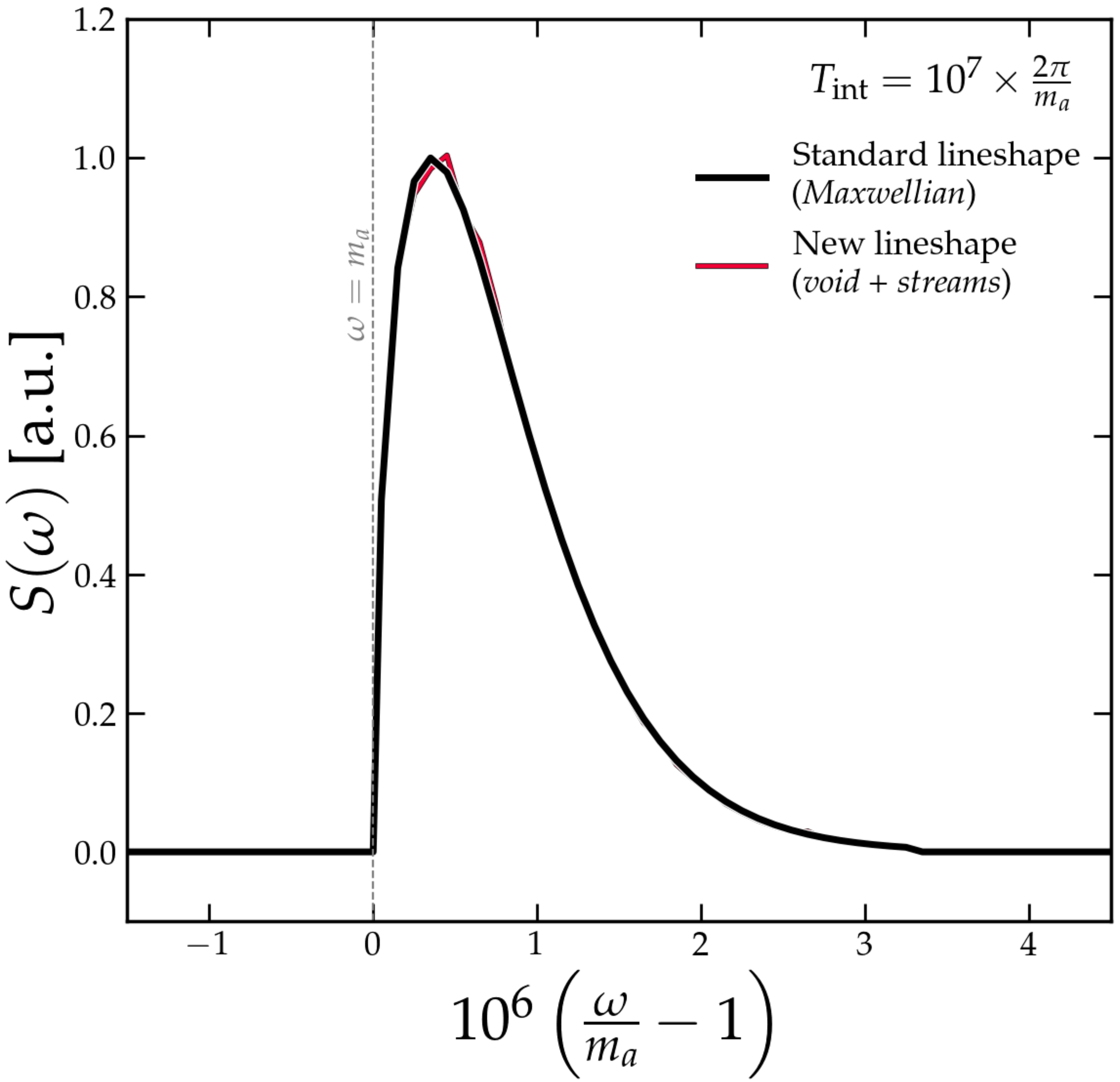

Haloscope signal

Disrupted minicluster **streams** are extremely cold ($\sigma < 1$ km/s) and do not contribute a significant density enhancement. However they become extremely prominent if lineshape is sufficiently well-resolved (long integration times)

Signal $S(\omega) \propto$ discrete FT of timestream

Frequency resolution = $\Delta\omega \sim T_{\rm int}^{-1}$

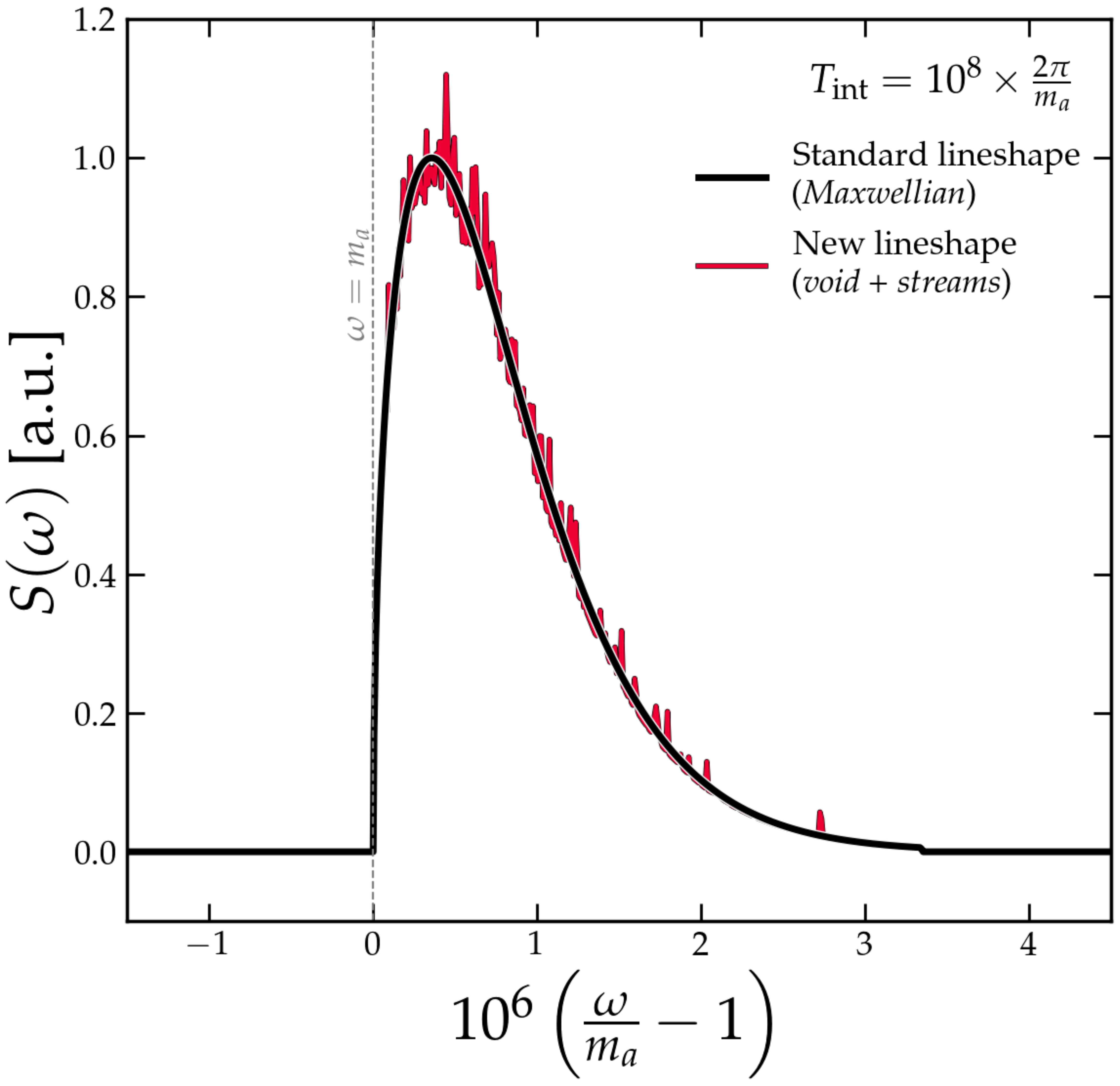

Haloscope signal

Disrupted minicluster **streams** are extremely cold ($\sigma < 1$ km/s) and do not contribute a significant density enhancement. However they become extremely prominent if lineshape is sufficiently well-resolved (long integration times)

Some important observations:

- Streams only enhance the signal by $\rho_{\rm str}/\rho_{\rm void} \sim 7$, but can enhance it by many orders of magnitude more in the *resolved* lineshape in certain bins
- Many streams are narrower than daily modulation in lab motion $v \sim 0.47$ km/s
- Streams persist in lineshape $\mathcal{O}$(days-years) at a time

Signal $S(\omega) \propto$ discrete FT of timestream

Frequency resolution = $\Delta\omega \sim T_{\rm int}^{-1}$

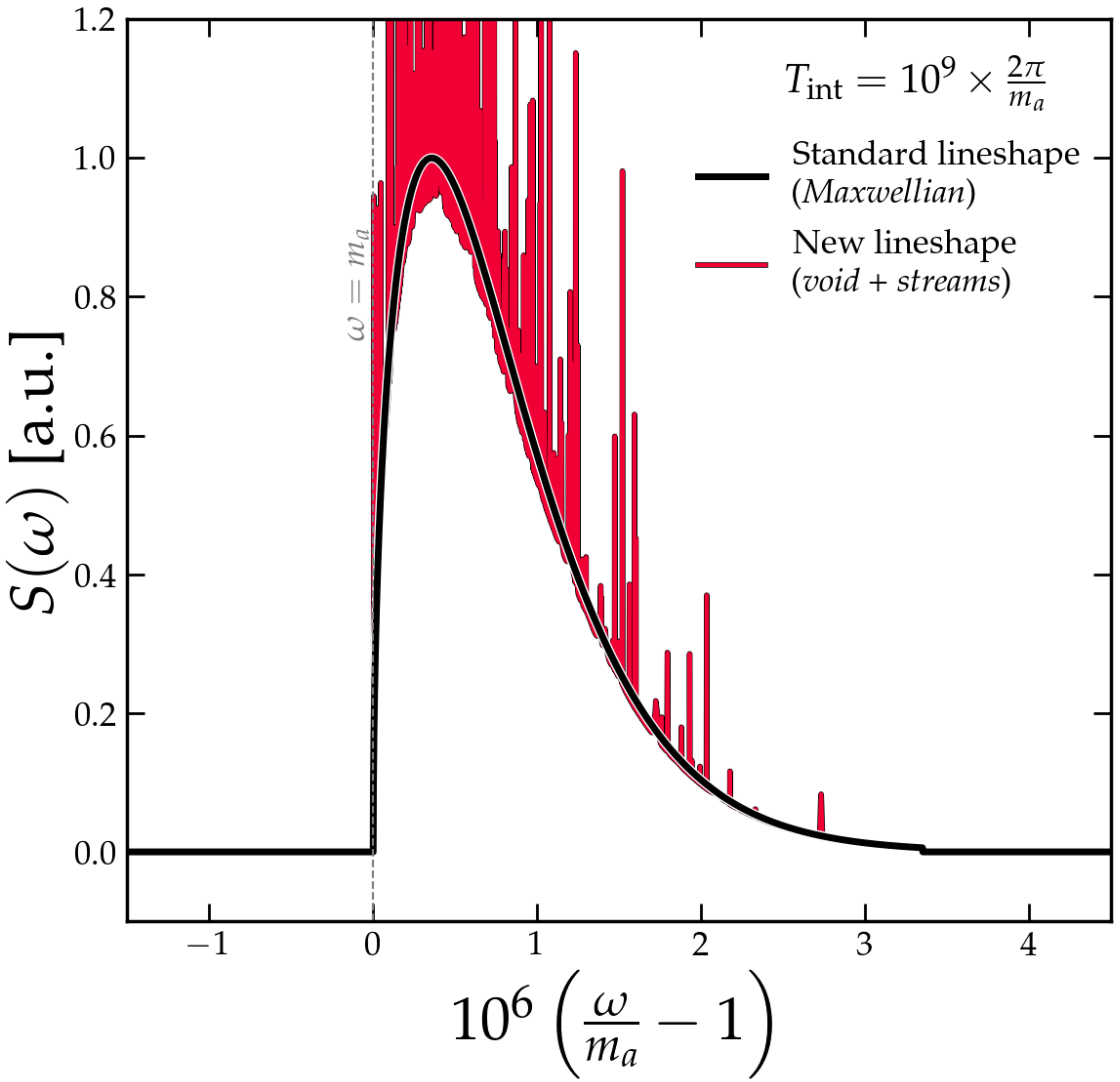

Summary

- **Miniclusters, voids and streams** are a *consequence* of the post-inflationary axion dark matter scenario so any observational/experimental test of this scenario must account for them to be self-consistent
- Ignoring tidal disruption, the worst-case scenario is that we are in a minivoid which has only about ~10% $\rho_{\rm DM}$ (suppression in $g_{a\gamma}$ sensitivity by a factor of 3)
- Accounting for tidal disruption, phase space at Solar position re-filled by a factor of 6, to about 70% of $\rho_{\rm DM}$ (suppression in $g_{a\gamma}$ by a factor of 1.2)
- $\mathcal{O}$(1000) ultra-cold tidal streams present in axion lineshape at any one time that persist for $\mathcal{O}$(days—years) at a time